Bethe stopping-power formula and its corrections

Francesc Salvat *

Facultat de Física, FQA and ICC, Universitat de Barcelona, Diagonal 645, 08028 Barcelona, Catalonia, Spain

(Received 10 May 2022; accepted 29 August 2022; published 19 September 2022)

The classical and quantum theories leading to the asymptotic Bethe formula of the stopping power of matter for charged particles heavier than the electron are briefly reviewed. Models and approximations for the practical calculation of various corrections that extend the validity range of the formula are described. The asymptotic formula and the associated shell correction were determined previously from an extensive database of atomic generalized oscillator strengths, calculated for an independent-electron model with the Dirac-Hartree-Fock-Slater (DHFS) self-consistent potential, with due account for relativistic departures from the Bethe sum rule. The nonrelativistic Bloch correction is extended to the relativistic domain by means of the Lindhard-Sørensen formulation, and an accurate parametrization for point projectiles with small charges is proposed. The density-effect correction and the Barkas correction are obtained from a semiempirical model of the optical oscillator strength (OOS), built from the calculated DHFS contributions of inner electron subshells plus the OOS of outer-shell electrons represented by an analytical expression, which is determined by the composition, mass density, and empirical mean excitation energy, or I value of the material. Inclusion of the shell, density-effect, Lindhard-Sørensen, and Barkas corrections into the asymptotic formula leads to the corrected Bethe formula. A general strategy is proposed to determine the stopping power in terms of only the I value of the material. It is shown that, with the empirical I values recommended in Report 37 of the International Commission on Radiation Units and Measurements, the stopping powers calculated numerically from the corrected formula are in close agreement with available measurements of the stopping power of elemental materials for protons and alpha particles with energies higher than 0.75 and 5 MeV, respectively.

DOI: 10.1103/PhysRevA.106.032809

I. INTRODUCTION

A fast charged particle in matter loses energy through interactions of different kinds, namely, (1) inelastic collisions, i.e., interactions that produce electronic excitations of the material (electronic stopping); (2) elastic collisions, which cause the recoil of the target atom (nuclear stopping); and (3) the emission of bremsstrahlung, or breaking radiation (radiative stopping). The present paper is focused on the electronic stopping of materials for charged particles heavier than the electron with kinetic energies up to about ten times their rest energy, for which the effect of nuclear stopping is small and that of radiative stopping is negligible.

The theory of electronic stopping has attracted a good deal of interest for longer than a century. Its main result is the celebrated Bethe formula for the stopping power, which gives the average energy loss per unit path length of the projectile. In principle, the Bethe formula is asymptotic, i.e., valid for projectiles with sufficiently high kinetic energy, and applicable only to thin atomic or molecular gases. Various correction terms need to be introduced to extend the validity of the formula down to intermediate energies and to dense materials. The present paper is intended to present in a unified manner the basic theoretical considerations leading to the Bethe formula and to its corrections, to identify the empirical information necessary for quantitative purposes, and to assess the range of validity of the formula by comparison with measured stopping-power data.

A summary description is given of the various derivations of the Bethe formula, following essentially the historical order in which they were developed. The classical approach of Bohr [1,2], slightly modified to account for relativistic kinematics, is presented in Sec. II. Section III deals with the quantum perturbation method of Bethe [3,4]. The classical and quantum approaches are consistent, in the sense that they lead to the same stopping-power formula for low-density materials, in which the characteristics of the medium enter through a pair of parameters, the average electron density, and the mean excitation energy I, which is defined as an integral property of the optical oscillator strength (OOS).

The quantum theory of stopping is based on the relativistic plane-wave Born approximation (PWBA), a first-order perturbative approach, which is described, e.g., by Fano [5]. The central result from the PWBA (Sec. III) for collisions with individual atoms or molecules is a closed expression for the doubly differential cross section (DDCS, differential in the energy loss W and the recoil energy Q) in terms of kinematical factors and the longitudinal and transverse generalized

*francesc.salvat@ub.edu

oscillator strengths (GOSs). The stopping-power formula is obtained from considerations based on (1) the global features of the GOSs; (2) the Bethe sum rule, which asserts that the integral over the energy loss of the GOS with a fixed value of Q equals the number of bound electrons in the target atom or molecule, irrespective of the Q value; and (3) the assumption that the energy of the projectile is sufficiently high to permit the simplification of certain integrals of the GOS. Originally, PWBA calculations were performed analytically by using simple hydrogenic atomic models (see, e.g., Ref. [6]). These calculations provided qualitative knowledge on the GOS of atomic and molecular targets, and allowed the formal derivation of the Bethe formula. Calculations with more elaborated atomic models, which require massive numerical computations, have been possible only since the 1990's. A systematic calculation of the GOSs for the electron subshells of neutral atoms in their ground-state configuration, based on the independent-electron model with the self-consistent Dirac-Hartree-Fock-Slater (DHFS) potential, was performed by Bote and Salvat [7] and by Salvat *et al.* [8]. The numerical GOSs exhibit a well-known departure from the Bethe sum rule caused by relativistic effects. Proper consideration of this departure implies a formal modification of the asymptotic formula for the stopping cross section, and it allows determining an atomic shell correction that, when added to the asymptotic formula, reproduces the stopping cross section obtained by numerical integration of the DDCS [8]. As the main contributions to the shell correction originate from excitations of inner electron subshells, which are expected to be described realistically by the DHFS model, the shell correction calculated for free atoms should also be approximately valid for dense materials and compounds.

Fermi [9] noted that the stopping power of a dense material for fast charged particles is smaller than that of a thin gas of the same composition due to the dielectric polarization of the medium caused by the electromagnetic field of the projectile. The semiclassical dielectric formulation [9–11] sketched in Sec. IV, which is shown to be equivalent to the quantum formulation for low-density materials, allows deriving a generic method for computing the density-effect correction to the stopping power in terms of the OOS of the material. In the case of high-energy projectiles, the dielectric polarization can be accounted for by adding a correction term to the asymptotic Bethe formula [12,13].

The validity of the formula can be extended to lower energies by adding additional correction terms. At intermediate energies, a correction is required to account for the difference between the stopping power predicted by the asymptotic formula and the result from a numerical integration of the DDCS obtained from the PWBA. This is the shell correction mentioned above. Bloch [14] pointed out that the classical calculation by Bohr would be more reliable than the PWBA for slow heavy projectiles, and derived a correction term to the nonrelativistic Bethe formula which yields stopping powers that approach the values obtained from Bohr's formula when the latter is superior. The Bloch nonrelativistic correction is introduced in Sec. V by following the derivation of Lindhard and Sørensen [15], which allows extending the correction to the relativistic domain. Finally, observed small differences between the stopping powers for particles with the same speeds and masses but opposite charges are accounted for by the so-called Barkas-effect correction, which is described in Sec. VI as a modification of Bohr's classical formulation for the distant interactions by introducing (to lowest order) the spatial variation of the electric field of the projectile within the volume swept by the oscillating target electrons [16,17].

The corrected Bethe formula, obtained by combining the asymptotic formula for the stopping cross section of individual atoms or molecules, the DHFS shell correction, the density-effect correction, the Lindhard-Sørensen correction, and the Barkas correction, is presented in Sec. VII. Because the density-effect and Barkas corrections are calculated from the OOS of the material, in Sec. VIII we consider various alternative models of the OOS and justify the use of an empirical OOS model based on atomic subshell OOSs calculated with the DHFS potential. With that empirical OOS, the corrected Bethe formula contains only two parameters: the effective mean excitation energy I_0', and the cutoff impact parameter a for distant interactions, which determines the Barkas correction.

The consistency of the theory is analyzed in Sec. IX by comparing the predictions of the corrected Bethe formula with experimental data. For this purpose we use measured stopping powers for protons and alpha particles taken from the exhaustive International Atomic Energy Agency (IAEA) online database [18] on "Electronic Stopping Power of Matter for Ions" [19]. A preliminary comparison of measured stopping powers and the prediction of the corrected Bethe formula, with the DHFS-model OOS and parameters estimated from empirical arguments, indicated that the formula is valid (i.e., it yields the approximate energy dependence of the measured stopping powers) for protons and alphas with kinetic energies higher than about 0.75 and 5 MeV, respectively.

An attempt to obtain the parameters I_0' and a by fitting the measurements leads to the conclusion that experimental uncertainties hide the tendency needed for an unambiguous fit. In that situation, we relaxed our requirements by considering that the I_0' parameter can be identified with the empirical I values recommended in the International Commission on Radiation Units and Measurements (ICRU) Report 37 [20], which were determined using information from multiple sources, and by estimating the value of the cutoff impact parameter a empirically on the basis of the limited information gained from the fits. With these parameters, we found generally good agreement between the corrected Bethe formula and the experiments in the energy range where the formula is expected to be valid. We present a graphical comparison of the IAEA stopping powers with the prediction of the corrected Bethe formula for 18 elements for which enough experimental information in the relevant energy range was available for both protons and alphas. A similar comparison for all the other elements included in the IAEA database is given in the Supplemental Material [21], which confirms that results from the corrected Bethe formula obtained with the proposed calculation scheme are consistent with experimental stopping-power data. The document ends with a few concluding comments given in Sec. X. A computer program that calculates the stopping power of arbitrary materials for point charged particles from the corrected Bethe formula, together with the required database of DHFS-model OOSs and atomic

shell corrections, is provided as part of the Supplemental Material [21].

For concreteness, we limit the presentation of the theory to homogeneous elemental materials, although, with minor modifications, the corrected Bethe formula [Eq. (128)] is also valid for alloys and compounds. We consider a fast charged projectile (mass $M_1 \gg m_e$ and charge $Z_1 e$, with m_e and e denoting the electron mass and the elementary charge, respectively) that moves with kinetic energy E in an elemental material of atomic number Z with $\mathcal{N}$ atoms per unit volume. To cover the energy range of interest, relativistic kinematics is used thorough the text. We recall that the kinetic energy E and the magnitude p of the linear momentum of the projectile can be expressed as

$$E = (\gamma - 1)M_1 c^2, \quad p = \beta\gamma M_1 c, \tag{1}$$

where

$$\beta = \frac{v}{c} = \sqrt{\frac{\gamma^2 - 1}{\gamma^2}} = \sqrt{\frac{E(E + 2M_1 c^2)}{(E + M_1 c^2)^2}} \tag{2}$$

is the projectile's velocity v in units of the speed of light c, and

$$\gamma = \sqrt{\frac{1}{1 - \beta^2}} = \frac{E + M_1 c^2}{M_1 c^2} \tag{3}$$

is the total energy of the projectile in units of its rest energy. Notice that

$$cp = \sqrt{E(E + 2M_1 c^2)}. \tag{4}$$

Each inelastic interaction involves a certain energy transfer W from the projectile to the medium. Inelastic "collisions" are characterized by the atomic energy-loss differential cross section (DCS), $d\sigma/dW$, from which we can calculate the atomic total cross section, $\sigma^{(0)}$, and the stopping cross section, $\sigma^{(1)}$, as integrals of the DCS:

$$\sigma^{(n)} = \int_0^E W^n \frac{d\sigma}{dW}\, dW. \tag{5}$$

The stopping power S is defined as the average energy loss per unit path length s of the projectile. It can be evaluated as the ratio of the average energy loss in a collision,

$$\langle W \rangle = \int_0^E W \frac{1}{\sigma^{(0)}} \frac{d\sigma}{dW}\, dW, \tag{6}$$

and the mean free path for inelastic interactions, $\lambda = (\mathcal{N}\sigma^{(0)})^{-1}$, that is,

$$S \equiv -\frac{dE}{ds} = \frac{\langle W \rangle}{\lambda} = \mathcal{N}\sigma^{(1)}. \tag{7}$$

Very often the terms "stopping power" and "stopping cross section" are used interchangeably.

II. CLASSICAL THEORY OF STOPPING

The first formula for the electronic stopping power was derived by Bohr [1,2] from purely classical arguments. Bohr's approach is not only of historical interest, for it is also the basis of the derivation of the Lindhard-Sørensen and Barkas corrections (see Secs. V and VI).

The starting point of Bohr's calculation was the DCS for classical nonrelativistic collisions of a projectile moving with velocity **v** with an electron at rest, assuming that they interact through the Coulomb force. In the center-of-mass (c.m.) frame these binary collisions are described by the Rutherford DCS:

$$\frac{d\sigma_{\rm cl}}{d\Omega} = \left(\frac{Z_1 e^2}{2m_e v^2}\right)^2 \frac{1}{\sin^4(\theta/2)}, \tag{8}$$

where v is the relative velocity and θ is the scattering angle in the c.m. frame. The angle θ and the impact parameter b (defined as the distance from the initial position of the target electron to the undisturbed straight trajectory of the projectile) are related by

$$\sin^2(\theta/2) = \frac{(Z_1 e^2/m_e v^2)^2}{b^2 + (Z_1 e^2/m_e v^2)^2}. \tag{9}$$

The Rutherford DCS is valid (i.e., coincident with the DCS obtained from an exact quantum calculation) when the absolute value of the Sommerfeld parameter

$$\eta \equiv \frac{Z_1 e^2}{\hbar v} \tag{10}$$

is much larger than unity [22]. $\hbar = h/(2\pi)$ is the reduced Plank constant.

As a consequence of disregarding relativistic effects, Bohr's original formula misses part of the relativistic terms in the Bethe formula, Eq. (40) below (see, e.g., Ref. [23]). To get the correct relativistic form of the stopping-power formula, we slightly modify Bohr's reasoning by following an argument first proposed by Fermi and further developed by Jackson and McCarthy [17]. We limit our considerations to projectiles much heavier than the electron ($M_1 \gg m_e$), so that the c.m. frame practically coincides with the rest frame of the projectile, and the velocity of the electron in the c.m. frame is $\simeq -\mathbf{v}$. As discussed by Jackson and McCarthy, the c.m. DCS is essentially the same as the DCS for scattering of an electron that moves with speed v in the Coulomb potential of the projectile; this approach is also adopted by Lindhard and Sørensen [15]. The scattering of an electron by a fixed-point charge $Z_1 e$ is described by the Mott DCS [24,25], which is obtained from the exact solution of the Dirac equation for the Coulomb potential. We consider the McKinley and Feshbach [26] expansion of the Mott DCS:

$$\frac{d\sigma_{\rm M2}}{d\Omega} = \left(\frac{Z_1 e^2}{2vp}\right)^2 \frac{1}{\sin^4(\theta/2)}\{1 - \beta^2 \sin^2(\theta/2) + \pi Z_1 \alpha\beta \sin(\theta/2)\,[1 - \sin(\theta/2)]\}, \tag{11}$$

where $p = \beta\gamma m_e c$ is the momentum of an electron moving with the speed of the projectile, and $\alpha = e^2/\hbar c \approx 1/137$ is the fine-structure constant. The relativistic correction that is missing in Bohr's stopping-power formula is obtained by using relativistic kinematics and by replacing the Rutherford DCS (8) with the two first terms in Eq. (11):

$$\frac{d\sigma_{\rm M1}}{d\Omega} = \left(\frac{Z_1 e^2}{2vp}\right)^2 \frac{1}{\sin^4(\theta/2)}[1 - \beta^2 \sin^2(\theta/2)]. \tag{12}$$

This expression is also obtained from the Born approximation for spin-$\frac{1}{2}$ particles (see, e.g., Ref. [25]). Since the spin

correction, $-\beta^2\sin^2(\theta/2)$, decreases in magnitude when the scattering angle decreases, the equality (9) with the electron relativistic mass γm_e,

$$\sin^2(\theta/2) = \frac{(Z_1e^2/\gamma m_e v^2)^2}{b^2 + (Z_1e^2/\gamma m_e v^2)^2}, \tag{13}$$

still holds valid for impact parameters that are sufficiently large (i.e., for small scattering angles in the c.m. frame).

After the binary collision, the target electron recoils with the kinetic energy

$$W = W_{\max}\,\sin^2(\theta/2) = W_{\max}\,\frac{1-\cos\theta}{2}, \tag{14}$$

where

$$\begin{aligned} W_{\max} &= \frac{2\beta^2\gamma^2\, m_e c^2}{1 + 2(m_e/M_1)\gamma + (m_e/M_1)^2} \\ &\simeq 2\beta^2\gamma^2\, m_e c^2 \end{aligned} \tag{15}$$

is the largest allowed energy transfer in a collision. Hence, the energy-loss DCS for collisions with an electron at rest is

$$\begin{aligned} \frac{d\sigma_{\rm M1}}{dW} &= \frac{2\pi\,\sin\theta\, d\theta}{dW}\,\frac{d\sigma_{\rm M1}}{d\Omega} \\ &= \frac{2\pi Z_1^2 e^4}{m_e v^2}\,\frac{1}{W^2}\left(1 - \beta^2\frac{W}{W_{\max}}\right), \end{aligned} \tag{16}$$

which differs from the DCS adopted by Bohr in that (1) $v = \beta c$ is the relativistic velocity and (2) it includes the spin correction. Equations (13) and (14) imply the following relationship between the energy loss and the impact parameter b:

$$W(b) = W_{\max}\,\frac{b_{\min}^2}{b^2 + b_{\min}^2} \tag{17}$$

with

$$b_{\min} = \frac{Z_1 e^2}{\beta^2\gamma m_e c^2}. \tag{18}$$

Bohr noticed that bound electrons with large impact parameters would feel the electric field of the projectile varying slowly with time and, consequently, they would respond adiabatically (that is, their orbits would stretch slowly as the projectile approaches and gently return to their original shapes when the projectile moves away) without absorbing any energy (see, e.g., Ref. [27]). This feature sets an upper adiabatic limit, $b_{\rm ad}$, to the impact parameters of electrons that effectively contribute to the stopping. The precise value of $b_{\rm ad}$ can only be determined from a comparison of calculated results with available experimental data.

A. Close collisions

The contribution to the stopping power of electrons with impact parameter less than a certain cutoff value a (assumed to be less than $b_{\rm ad}$) is given by

$$\begin{aligned} S_{{\rm cl},b<a} &= \mathcal{N}Z\int_{W(a)}^{W_{\max}} W\,\frac{d\sigma_{\rm M1}}{dW}\,dW \\ &= \frac{2\pi Z_1^2 e^4}{m_e v^2}\,\mathcal{N}Z\Big[\ln W - \beta^2\frac{W}{W_{\max}}\Big]_{W(a)}^{W_{\max}}. \end{aligned} \tag{19}$$

For projectiles with sufficiently large velocities, we can select a value of the cutoff impact parameter a such that $a \gg b_{\min}$ [see Eq. (18)], and write

$$\begin{aligned} S_{{\rm cl},b<a} &= \frac{2\pi Z_1^2 e^4}{m_e v^2}\,\mathcal{N}Z\left[2\,\ln\left(a\,\frac{\gamma\, m_e v^2}{|Z_1|e^2}\right) - \beta^2\right] \\ &= \frac{4\pi Z_1^2 e^4}{m_e v^2}\,\mathcal{N}Z\left[\ln\left(a\,\frac{m_e v^2}{|Z_1|e^2}\right) + \frac{1}{2}\ln\gamma^2 - \frac{1}{2}\,\beta^2\right]. \end{aligned} \tag{20}$$

The first term in this expression coincides with Bohr's nonrelativistic result; the second and third terms give the correct relativistic correction obtained from the PWBA [see Eq. (40)].

B. Distant interactions

The need for determining the adiabatic impact parameter $b_{\rm ad}$ is avoided if the contribution of distant interactions with $b > a$ is calculated by treating the electrons as classical oscillators. The energy transferred to a harmonically bound electron at a distance b from the trajectory of the passing projectile is given by [Eq. (13.31) of Ref. [11]]

$$W(b,\omega) = \frac{2Z_1^2 e^4}{m_e v^2}\,\frac{1}{b^2}\left[\xi^2 K_1^2(\xi) + \frac{1}{\gamma^2}\xi^2 K_0^2(\xi)\right], \tag{21}$$

where ω is the binding angular frequency of the oscillator, $K_n(x)$ are modified Bessel functions of orders $n = 0$ and 1 [28], and

$$\xi = \frac{\omega b}{\gamma v}. \tag{22}$$

In the derivation of Eq. (21), it is assumed that the electric field of the projectile is uniform over the volume swept by the trajectory of the oscillating electron, similarly to the dipole approximation employed in atomic physics (see, e.g., Ref. [29]).

A basic ingredient of the classical theory is the oscillator strength density, $df(\omega)/d\omega$. The quantity $[df(\omega)/d\omega]\,d\omega$ is defined as the number of atomic electrons having harmonic binding frequency ω in the interval $(\omega, \omega + d\omega)$. Naturally, the oscillator strength density is assumed to satisfy the sum rule

$$\int_0^\infty \frac{df(\omega)}{d\omega}\,d\omega = Z. \tag{23}$$

The contribution to the stopping power of oscillators with impact parameters larger than a given cutoff value a is

$$\begin{aligned} S_{{\rm cl},b>a} &= 2\pi\mathcal{N}\int_0^\infty d\omega\,\frac{df(\omega)}{d\omega}\int_a^\infty W(b,\omega)\,b\,db \\ &= \frac{4\pi Z_1^2 e^4}{m_e v^2}\,\mathcal{N}\int_0^\infty d\omega\,\frac{df(\omega)}{d\omega} \\ &\quad\times\int_{\xi_a}^\infty\left[K_1^2(\xi) + \frac{1}{\gamma^2}K_0^2(\xi)\right]\xi\,d\xi \end{aligned} \tag{24}$$

with $\xi_a = \omega a/(\gamma v)$. Since the integrand decreases rapidly to zero for large b, the upper limit of the second integral has been set to ∞. The integral over ξ can be solved in closed form

giving [Eq. (13.35) of Ref. [11]]

$$S_{\mathrm{cl},b>a} = \frac{4\pi Z_1^2 e^4}{m_e v^2}\mathcal{N}\int_0^\infty d\omega\,\frac{df(\omega)}{d\omega}\Big[\xi_a K_1(\xi_a)K_0(\xi_a) - \frac{v^2}{2c^2}\xi_a^2\big[K_1^2(\xi_a)-K_0^2(\xi_a)\big]\Big]. \tag{25}$$

In situations of practical interest with high-energy particles (see below) $\xi_a \ll 1$ and we can use the small-argument forms of the Bessel functions [28] to simplify the last expression. We have

$$S_{\mathrm{cl},b>a} = \frac{4\pi Z_1^2 e^4}{m_e v^2}\mathcal{N}\int_0^\infty d\omega\,\frac{df(\omega)}{d\omega} \times\left[\ln\left(\frac{2\exp(-g)\gamma v}{a\omega}\right)-\frac{v^2}{2c^2}\right], \tag{26}$$

where $g = 0.5772$ is Euler's constant. Using the sum rule (23), we can write

$$S_{\mathrm{cl},b>a} = \frac{4\pi Z_1^2 e^4}{m_e v^2}\mathcal{N}Z\left[\ln\left(\frac{2\exp(-g)\,v}{a\overline{\omega}}\right)+\frac{1}{2}\ln\gamma^2-\frac{1}{2}\beta^2\right], \tag{27}$$

where $\overline{\omega}$ is an average binding frequency defined by

$$\ln\overline{\omega} = \frac{1}{Z}\int_0^\infty \ln(\omega)\,\frac{df(\omega)}{d\omega}\,d\omega. \tag{28}$$

The classical stopping power S_{cl} is the sum of contributions from close and distant collisions:

$$S_{\mathrm{cl}} = S_{\mathrm{cl},b<a} + S_{\mathrm{cl},b>a}.$$

We thus obtain the classical high-energy (asymptotic) formula

$$S_{\mathrm{Bohr}} = \frac{4\pi Z_1^2 e^4}{m_e v^2}\mathcal{N}Z\left[\ln\left(\frac{2\exp(-g)\,m_e v^3}{|Z_1|\,e^2\,\overline{\omega}}\right)+\ln\gamma^2-\beta^2\right], \tag{29}$$

which, aside from the contribution of close collisions to the relativistic correction $[=\frac{1}{2}(\ln\gamma^2-\beta^2)]$, coincides with Bohr's classical stopping-power formula. It is interesting to observe that the only characteristics of the material entering this formula are the total average electron density $\mathcal{N}Z$ and the average binding frequency $\overline{\omega}$.

III. THE QUANTUM THEORY OF BETHE

The nonrelativistic quantum theory of inelastic collisions of charged projectiles with atoms was first formulated by Bethe [3] on the basis of the PWBA, in which the projectile states are represented as plane waves and the interaction between the projectile and the target electrons is treated as a perturbation to first order. The theory was subsequently extended to the relativistic domain by Bethe [4] and Møller [30]. General considerations [6] indicate that the PWBA is expected to be valid (i.e., giving results in agreement with those from an exact quantum calculation) when $Z\alpha \ll \beta$.

In its original form, the relativistic Bethe theory considers inelastic collisions of a projectile with initial kinetic energy E and linear momentum $\mathbf{p}$ with a neutral atom of the element of atomic number Z in its ground state. Let E' and $\mathbf{p}'$ denote the kinetic energy and momentum of the projectile after the collision. The effect of the interaction on the projectile is described by a DDCS that depends on the energy loss $W = E - E'$ and the polar scattering angle θ, i.e., the angle between $\mathbf{p}$ and $\mathbf{p}'$. A reformulation of the theory by Fano [5], using electromagnetic potentials in the Coulomb gauge (see, e.g., Ref. [11]), shows that the DDCS takes a more intelligible form when the polar scattering angle is replaced with the recoil energy Q defined as the kinetic energy of an electron with linear momentum equal to the momentum transfer $\hbar\mathbf{q} = \mathbf{p} - \mathbf{p}'$, i.e., such that

$$Q(Q+2m_e c^2) \equiv (c\hbar q)^2 = c^2(p^2+p'^2-2pp'\cos\theta) \tag{30}$$

or

$$Q = \sqrt{(c\hbar q)^2 + m_e^2 c^4} - m_e c^2. \tag{31}$$

For a given energy loss W, the allowed values of Q lie in the interval (Q_-, Q_+) with

$$Q_\pm = \sqrt{(cp \pm cp')^2 + m_e^2 c^4} - m_e c^2. \tag{32}$$

For projectiles with high energy and $W \ll E$,

$$Q_- \simeq \frac{W^2}{2\beta^2 m_e c^2}. \tag{33}$$

The DCS obtained from the PWBA can be expressed as (see Refs. [5,8])

$$\frac{d^2\sigma}{dQ\,dW} = \frac{2\pi Z_1^2 e^4}{m_e v^2}\left[\frac{2m_e c^2}{WQ(Q+2m_e c^2)}\frac{df(Q,W)}{dW} + \beta^2\left(1-\frac{W^2}{\beta^2 Q(Q+2m_e c^2)}\right)\frac{2m_e c^2 W}{[Q(Q+2m_e c^2)-W^2]^2}\frac{dg(Q,W)}{dW}\right], \tag{34}$$

where the functions $df(Q,W)/dW$ and $dg(Q,W)/dW$ are, respectively, the longitudinal and transverse GOSs, which are defined in terms of matrix elements of the effective interaction Hamiltonian (see Ref. [5]) between initial and final states of the projectile and the target atom. The longitudinal GOS accounts for the response of the target atom to the instantaneous Coulomb potential of the projectile, while the transverse DCS describes the effect of transverse interactions (i.e., exchange of virtual photons between the projectile and the atom). The contribution of transverse interactions vanishes in the nonrelativistic limit ($c \to \infty$, $\beta \to 0$), in which the DDCS reduces to

$$\frac{d^2\sigma}{dQ\,dW} = \frac{2\pi Z_1^2 e^4}{m_e v_{\mathrm{NR}}^2}\frac{1}{WQ}\frac{df_{\mathrm{NR}}(Q,W)}{dW}, \tag{35}$$

with the nonrelativistic speed of the projectile, $v_{\mathrm{NR}}^2 = 2E/M_1$.

Although the nonrelativistic GOS of the hydrogen atom and one-electron ions can be expressed in closed analytical form [6], relativistic GOSs have to be calculated numerically. The most elaborate calculations available [8] are based on a relativistic independent-electron model, in which atomic states are represented as single Slater determinants built with one-electron orbitals that are solutions of the Dirac equation with the DHFS self-consistent potential for the ground-state configuration of the target atom (see, e.g., Ref. [31]). This atomic model is hereafter referred to as the DHFS model. The GOSs obtained from it are expressed as sums of contributions from the electron subshells of the ground-state configuration, that is,

$$\frac{df(Q,W)}{dW} = \sum_i \frac{df_i(Q,W)}{dW},$$
$$\frac{dg(Q,W)}{dW} = \sum_i \frac{dg_i(Q,W)}{dW}. \tag{36}$$

The GOSs $df_i(Q,W)/dW$ and $dg_i(Q,W)/dW$ of the ith subshell with ionization energy U_i can be calculated to high numerical accuracy. They consist of a continuum of energy transfers W higher than U_i, which correspond to transitions of individual electrons to final orbitals with positive energy (ionization), and a set of discrete resonances with excitation energies below U_i that represent excitations of electrons to bound orbitals. Salvat *et al.* [8] used a computer code developed by Bote and Salvat [7] to generate a complete database of GOSs for all the subshells of the ground-state configurations of neutral atoms of the elements from hydrogen ($Z = 1$) to einsteinium ($Z = 99$). These calculated GOSs are expected to provide a realistic description of the response of electrons in inner subshells, but not for the outer subshells, which are sensitive to electron-correlation effects (neglected by the DHFS model) and, for compounds and condensed materials, to the state of aggregation.

The graphical representation of the GOS as a function of Q and W is called the Bethe surface [6]. A conspicuous feature of the Bethe surface is that, for Q larger than about $10\,U_i$, the subshell GOS reduces to a ridge, the Bethe ridge, that peaks near the line $W = Q$. In collisions with large momentum transfers, or with recoil energies much larger than the ionization energy U_i, the effect of binding is small and the target electrons react as if they were free and at rest. Under these circumstances, the subshell GOSs can be approximated as

$$\frac{df_i(Q,W)}{dW} \simeq f_i\,\delta(Q-W),$$
$$\frac{dg_i(Q,W)}{dW} \simeq f_i\,\delta(Q-W), \tag{37a}$$

where f_i is the number of electrons in the ith subshell. In the optical limit, $Q = 0$, both the longitudinal and transverse GOSs reduce to the OOS:

$$\frac{df(0,W)}{dW} = \frac{dg(0,W)}{dW} = \frac{df(W)}{dW}. \tag{37b}$$

In the nonrelativistic theory, the GOS satisfies the Bethe sum rule

$$\int_0^\infty \frac{df_{\rm NR}(Q,W)}{dW}\,dW = Z \quad \forall Q, \tag{37c}$$

which at $Q = 0$ reduces to the dipole (or Thomas-Reiche-Kuhn) sum rule [29]. Relativistic GOSs present small departures from the Bethe sum rule that are disregarded in most generic studies (see Sec. VII).

Integration of the DDCS over recoil energies yields the energy-loss DCS:

$$\frac{d\sigma}{dW} = \int_{Q_-}^{Q_+} \frac{d^2\sigma}{dQ\,dW}\,dQ = \sum_i \frac{d\sigma_i}{dW}. \tag{38}$$

For sufficiently large recoil energies, the approximations (37a) are applicable and the subshell energy-loss DCS reduces to

$$\frac{d\sigma_i}{dW} = f_i\,\frac{2\pi Z_1^2 e^4}{m_e v^2}\,\frac{1}{W^2} \times\left(1-\beta^2\frac{W}{W_{\rm max}}+\frac{1-\beta^2}{2M_1^2c^4}\,W^2\right), \tag{39}$$

where $W_{\rm max}$ is the maximum energy transfer in a collision with free electrons at rest, which is given by Eq. (15). The total cross section, $\sigma^{(0)}$, and the stopping cross section, $\sigma^{(1)}$, are obtained as integrals of the energy-loss DCS [see Eq. (5)].

The global properties of the GOSs, Eqs. (37), allow deriving asymptotic formulas, valid for high-energy projectiles, for the total cross section and the stopping cross section (see, e.g., Ref. [5]). The asymptotic formula for the stopping cross section is known as the Bethe formula, which reads

$$\sigma^{(1)}_{\rm as,Bethe} = \frac{2\pi Z_1^2 e^4}{m_e v^2}\,2Z\left[\ln\left(\frac{2m_e v^2}{I}\right) + \ln\gamma^2 - \beta^2 + \frac{1}{2}\,f(\gamma)\right] \tag{40}$$

with the *mean excitation energy* I defined by

$$\ln I = \frac{1}{Z}\int_0^\infty \ln W\,\frac{df(W)}{dW}\,dW, \tag{41}$$

and

$$f(\gamma) = \ln(R) + \left(\frac{m_e}{M_1}\,\frac{\gamma^2-1}{\gamma}\,R\right)^2, \tag{42a}$$

where

$$R = [1 + (m_e/M_1)^2 + 2(m_e/M_1)\gamma]^{-1}. \tag{42b}$$

For particles much heavier than the electron, the quantity R is close to unity and $f(\gamma) \simeq 0$. We point out that the derivation of the formula (40) [5] makes explicit use of the Bethe sum rule (37c).

Because of the simplifications introduced in the derivation of the asymptotic formula (40), when the kinetic energy of the projectile is not large enough, the values given by that formula differ from the "exact" stopping cross section obtained by integrating the energy-loss DCS. The difference determines the *shell correction*, C/Z, which is defined in such a way that the corrected Bethe formula

$$\sigma^{(1)}_{\rm Bethe} = \frac{4\pi Z_1^2 e^4}{m_e v^2}\,Z\left[\ln\left(\frac{2m_e v^2}{I}\right) + \ln\gamma^2 - \beta^2 + \frac{1}{2}\,f(\gamma) - \frac{C(\gamma)}{Z}\right] \tag{43}$$

reproduces the calculated $\sigma^{(1)}$ values. Salvat *et al.* [8] have determined the shell correction for neutral atoms of the elements with $Z = 1$–99 and projectile protons with energies up to 10^{10} eV by using the GOSs calculated by means of the DHFS model. It is worth noticing that the stopping cross section obtained from the PWBA is determined by the speed and the squared charge of the projectile; it does not depend on either the mass or the sign of the charge of the projectile. This feature implies that the shell correction, considered as a function of γ, is valid for any kind of charged projectile much heavier than the electron. Electrons and positrons are affected by exchange and annihilation-recreation effects, which modify the terms $f(\gamma)$ and C/Z in the Bethe formula (see, e.g., Ref. [20]).

IV. SEMICLASSICAL DIELECTRIC THEORY

As indicated above, the PWBA describes inelastic interactions of the projectile with a free atom, that is, the asymptotic formula gives the stopping power, $S = \mathcal{N}\sigma^{(1)}$, of a low-density elemental gas. The stopping power of a condensed medium differs from that of a gas of the same composition because (1) the presence of neighboring atoms alters the wave functions of weakly bound and free electrons (aggregation effects) and (2) the material gets polarized by the electromagnetic field of the moving projectile (Fermi's density effect). A convenient framework for computing the stopping power of a condensed material is provided by the classical dielectric formalism [10,32], in which the material is described as a homogeneous and isotropic dielectric medium.

If the projectile charge is positive (negative), it attracts the electrons (nuclei) and repels the nuclei (electrons), polarizing the atoms of the medium. As the projectile is moving fast, the polarization is stronger behind the projectile than in front of it. This inhomogeneous polarization gives rise to an induced electric field $\boldsymbol{\mathcal{E}}_{\rm ind}$ that, in turn, produces a stopping force $Z_1 e\,\boldsymbol{\mathcal{E}}_{\rm ind}$ on the projectile. The stopping power, i.e., the average energy loss per unit path length, can then be identified with that force. Following Lindhard [10] the stopping power obtained from the classical dielectric approach can be expressed as

$$S_{\rm diel} = \frac{2Z_1^2 e^4}{\pi v^2}\int_0^\infty \omega\, d\omega \int_{\omega/v}^\infty \frac{dq}{q}\left[\mathrm{Im}\left(\frac{-1}{\epsilon^{(\mathrm{L})}(q,\omega)}\right) + \beta^2\left(1-\frac{\omega^2}{\beta^2c^2q^2}\right)\mathrm{Im}\left(\frac{1}{1-(\omega/cq)^2\,\epsilon^{(\mathrm{T})}(q,\omega)}\right)\right], \tag{44}$$

where $\epsilon^{(\mathrm{L})}(q,\omega)$ and $\epsilon^{(\mathrm{T})}(q,\omega)$ are, respectively, the longitudinal and transverse dielectric functions of the material, which depend on the wave number q and the angular frequency ω of the electromagnetic field. In the optical limit ($q = 0$), the two dielectric functions reduce to the optical dielectric function, $\epsilon(\omega)$:

$$\epsilon^{(\mathrm{L})}(0,\omega) = \epsilon^{(\mathrm{T})}(0,\omega) = \epsilon(\omega). \tag{45}$$

The classical dielectric approach describes the slowing down of a swift charged particle as a continuous process, while in reality the energy loss is the result of multiple discrete interactions. Semiclassical arguments (see, e.g., Ref. [11]) indicate that the variables ω and $\mathbf{q}$, which are introduced merely as variables of Fourier transformations, can be assigned a physical meaning by considering that $W = \hbar\omega$ and $\hbar\mathbf{q}$ represent, respectively, the energy loss and the momentum transfer in one interaction. In accordance with this interpretation, these variables are subject to the constraints of energy and linear momentum conservation. This semiclassical picture constitutes the link between the classical dielectric and quantum formulations. Indeed, in the case of thin atomic gases the dielectric formalism should be consistent with the results from PWBA calculations.

Let us express $S_{\rm diel}$ in terms of the single-interaction variables Q [Eq. (31)] and $W = \hbar\omega$. Assuming that $W \ll E$, the lower limit of the integral over Q is [see Eq. (33)]

$$\sqrt{(c\hbar\,\omega/v)^2 - m_{\rm e}^2c^4} - m_{\rm e}c^2 \simeq \frac{W^2}{2m_{\rm e}c^2\beta^2} \simeq Q_-. \tag{46}$$

In addition, the upper limits of the integrals can be replaced with $W_{\rm max}$ and Q_+, respectively, because the integrand tends to zero at large W or Q and, hence, it practically vanishes outside the kinematically allowed domain. We can thus write

$$S_{\rm diel} = \mathcal{N}\,\frac{2\pi Z_1^2 e^4}{m_{\rm e}v^2}\,\frac{2Z}{\pi(\hbar\Omega_{\rm p})^2}\int_0^{W_{\rm max}} dW\, W \int_{Q_-}^{Q_+} dQ\, \frac{2(Q+m_{\rm e}c^2)}{Q(Q+2m_{\rm e}c^2)}\left[\mathrm{Im}\left(\frac{-1}{\epsilon^{(\mathrm{L})}(Q,W)}\right)\right.$$
$$\left. + \beta^2\left(1-\frac{W^2}{\beta^2Q(Q+2m_{\rm e}c^2)}\right)\mathrm{Im}\left(1-\frac{W^2}{Q(Q+2m_{\rm e}c^2)}\,\epsilon^{(\mathrm{T})}(Q,W)\right)^{-1}\right], \tag{47}$$

where

$$\Omega_{\rm p} = \sqrt{4\pi\,\mathcal{N}Z\,\frac{e^2}{m_{\rm e}}} \tag{48}$$

is the plasma resonance frequency of an electron gas with the average electron density $\mathcal{N}Z$ of the medium.

To reveal the connection between the PWBA and the dielectric theory, we consider a low-density gas, for which $\mathrm{Re}(\epsilon^{(\mathrm{L,T})}) \simeq 1$ and $\mathrm{Im}(\epsilon^{(\mathrm{L,T})}) \ll 1$. The semiclassical expression (47) of the stopping power for such a material simplifies to

$$S_{\mathrm{diel},0} = \mathcal{N}\,\frac{2\pi Z_1^2 e^4}{m_\mathrm{e} v^2}\,\frac{2Z}{\pi(\hbar\Omega_\mathrm{p})^2}\int_0^{W_\mathrm{max}} dW\, W \int_{Q_-}^{Q_+} dQ \frac{2(Q+m_\mathrm{e}c^2)}{Q(Q+2m_\mathrm{e}c^2)}\left[\mathrm{Im}\left(\frac{-1}{\epsilon^{(\mathrm{L})}(Q,W)}\right)\right.$$
$$\left. + \beta^2\left(1-\frac{W^2}{\beta^2 Q(Q+2m_\mathrm{e}c^2)}\right)\frac{W^2 Q(Q+2m_\mathrm{e}c^2)}{[Q(Q+2m_\mathrm{e}c^2)-W^2]^2}\,\mathrm{Im}\left(\frac{-1}{\epsilon^{(\mathrm{T})}(Q,W)}\right)\right]. \tag{49}$$

We recall that in the PWBA, and in other quantal formulations, the stopping power is obtained as the following integral of the DDCS:

$$S = \mathcal{N}\int_0^{W_\mathrm{max}} dW\, W \int_{Q_-}^{Q_+} dQ\, \frac{d^2\sigma}{dQ\,dW}. \tag{50}$$

The similarity of these two expressions allows inferring the following formula for the semiclassical DDCS:

$$\frac{d^2\sigma_{\mathrm{diel},0}}{dQ\,dW} = \frac{2\pi Z_1^2 e^4}{m_\mathrm{e} v^2}\,\frac{2Z}{\pi(\hbar\Omega_\mathrm{p})^2}\,\frac{2(Q+m_\mathrm{e}c^2)}{Q(Q+2m_\mathrm{e}c^2)}\left[\mathrm{Im}\left(\frac{-1}{\epsilon^{(\mathrm{L})}(Q,W)}\right)\right.$$
$$\left. + \beta^2\left(1-\frac{W^2}{\beta^2 Q(Q+2m_\mathrm{e}c^2)}\right)\frac{W^2\,Q(Q+2m_\mathrm{e}c^2)}{[Q(Q+2m_\mathrm{e}c^2)-W^2]^2}\,\mathrm{Im}\left(\frac{-1}{\epsilon^{(\mathrm{T})}(Q,W)}\right)\right]. \tag{51}$$

Now, making the identifications

$$\frac{df(Q,W)}{dW} = W\,\frac{2Z}{\pi(\hbar\Omega_\mathrm{p})^2}\,\mathrm{Im}\left(\frac{-1}{\epsilon^{(\mathrm{L})}(Q,W)}\right) \tag{52a}$$

and

$$\frac{dg(Q,W)}{dW} = W\,\frac{2Z}{\pi(\hbar\Omega_\mathrm{p})^2}\,\mathrm{Im}\left(\frac{-1}{\epsilon^{(\mathrm{T})}(Q,W)}\right), \tag{52b}$$

we can write

$$\frac{d^2\sigma_{\mathrm{diel},0}}{dQ\,dW} = \frac{2\pi Z_1^2 e^4}{m_\mathrm{e} v^2}\left[\frac{2(Q+m_\mathrm{e}c^2)}{WQ(Q+2m_\mathrm{e}c^2)}\,\frac{df(Q,W)}{dW}\right.$$
$$\left. + \beta^2\left(1-\frac{W^2}{\beta^2 Q(Q+2m_\mathrm{e}c^2)}\right)\frac{2m_\mathrm{e}c^2\,W^2}{[Q(Q+2m_\mathrm{e}c^2)-W^2]^2}\,\frac{dg(Q,W)}{dW}\right]. \tag{53}$$

As this DDCS decreases rapidly with Q, we can replace the factor $Q+m_\mathrm{e}c^2$ in the numerator with $m_\mathrm{e}c^2$, and obtain a formula for the semiclassical DDCS that is identical to the result (34) from the relativistic PWBA.

Because the extension of the PWBA to dense materials is not feasible, we assume that the equivalence of the quantum perturbation theory and the semiclassical dielectric formalism, which we have just verified for thin gases, also holds for any amorphous material. Defining the longitudinal and transverse GOSs according to Eqs. (52), the semiclassical DDCS can be expressed as

$$\frac{d^2\sigma_{\mathrm{diel}}}{dQ\,dW} = \frac{d^2\sigma_{\mathrm{diel},0}}{dQ\,dW} + \frac{d^2(\Delta\sigma)_{\mathrm{pol}}}{dQ\,dW}. \tag{54}$$

The first term on the right-hand side represents the DDCS of an ideal "unpolarizable" material, in which the electromagnetic field of the projectile is the same as in vacuum. This term is formally identical to the result from the PWBA, except for the fact that now the GOSs pertain to the material. The second term,

$$\frac{d^2(\Delta\sigma)_{\mathrm{pol}}}{dQ\,dW} \equiv \frac{d^2\sigma_{\mathrm{diel}}}{dQ\,dW} - \frac{d^2\sigma_{\mathrm{diel},0}}{dQ\,dW} = \frac{2\pi Z_1^2 e^4}{m_\mathrm{e} v^2}\,\frac{2Z}{\pi(\hbar\Omega_\mathrm{p})^2}\,\frac{2m_\mathrm{e}c^2}{Q(Q+2m_\mathrm{e}c^2)}\,\beta^2\left(1-\frac{W^2}{\beta^2 Q(Q+2m_\mathrm{e}c^2)}\right)$$
$$\times\left[\mathrm{Im}\left(1-\frac{W^2}{Q(Q+2m_\mathrm{e}c^2)}\,\epsilon^{(\mathrm{T})}(Q,W)\right)^{-1} - \frac{W^2\,Q(Q+2m_\mathrm{e}c^2)}{[Q(Q+2m_\mathrm{e}c^2)-W^2]^2}\,\mathrm{Im}\left(\frac{-1}{\epsilon^{\mathrm{T}}(Q,W)}\right)\right], \tag{55}$$

can be regarded as a correction accounting for the effect of the dielectric polarization of the medium, the Fermi density effect.

The polarization correction is appreciable only for fast projectiles, with velocity v comparable to c (see Fig. 7 below), for which $Q_- \simeq W^2/(2m_\mathrm{e}c^2\beta^2)$ is much smaller than W ($Q_- \simeq 1$ eV for $W \simeq 1$ keV). Because the polarization correction (55) almost diverges at Q_-, the relevant recoil energies are small and, consequently, we can replace the dielectric functions on the right-hand side of Eq. (55) with their values at $Q = 0$. Thus, the polarization effect alters the DDCS only for low-Q transverse interactions and the correction is completely determined by the optical dielectric function. Heretofore, all calculations of the

density effect have utilized this approximation (see, e.g., Refs. [5,33,34]). With the Q dependence of the dielectric functions removed, Eq. (55) becomes

$$\frac{d^2(\Delta\sigma)_{\rm pol}}{dQ\,dW} = \frac{2\pi Z_1^2 e^4}{m_e v^2}\,\frac{2Z}{\pi(\hbar\Omega_p)^2}\,\frac{2(Q+m_e c^2)}{Q(Q+2m_e c^2)}\,\beta^2\left(1-\frac{W^2}{\beta^2 Q(Q+2m_e c^2)}\right) \times\left[{\rm Im}\left(1-\frac{W^2}{Q(Q+2m_e c^2)}\,\epsilon(W)\right)^{-1}-\frac{W^2\,Q(Q+2m_e c^2)}{[Q(Q+2m_e c^2)-W^2]^2}\,{\rm Im}\left(\frac{-1}{\epsilon(W)}\right)\right]. \tag{56}$$

Since this expression decreases rapidly with Q, the polarization correction to the stopping power can be calculated as

$$(\Delta S)_{\rm pol} = \mathcal{N}\int_0^{W_{\rm max}} dW\,W\int_{Q_-}^{\infty} dQ\,\frac{d^2(\Delta\sigma)_{\rm pol}}{dQ\,dW}, \tag{57}$$

where we have replaced the upper limit of the integral, Q_+, with infinity. Notice that, for projectiles with sufficiently high energies, the integrand decreases rapidly with W, and the upper limit $W_{\rm max}$ of the integral can be replaced with ∞.

Fano [12] derived a compact formula for the high-energy density-effect correction to the stopping power by using contour integration in the complex plane. He showed that

$$(\Delta S)_{\rm pol} = -\frac{2\pi Z_1^2 e^4}{m_e v^2}\,\mathcal{N}\,Z\,\delta_F \tag{58}$$

where δ_F is the *density effect correction*, which can be calculated as [13]

$$\delta_F \equiv \frac{1}{Z}\int_0^{\infty}\frac{df(W)}{dW}\ln\left(1+\frac{L^2}{W^2}\right)dW-\frac{L^2}{\hbar^2\Omega_p^2}(1-\beta^2), \tag{59}$$

where L is the positive root of the equation

$$\mathcal{F}(L)\equiv\frac{1}{Z}\hbar^2\Omega_p^2\int_0^{\infty}\frac{1}{W^2+L^2}\frac{df(W)}{dW}\,dW = 1-\beta^2. \tag{60}$$

The function $\mathcal{F}(L)$ decreases monotonically with L, and hence, the root $L(\beta^2)$ exists only when $1-\beta^2<\mathcal{F}(0)$; otherwise it is $\delta_F=0$. Therefore, the function $L(\beta^2)$ starts with zero at $\beta^2=1-\mathcal{F}(0)$ and grows monotonically with increasing β^2.

The stopping cross section of the unpolarizable medium for high-energy projectiles is given by the Bethe formula (43). The stopping cross section of the polarizable material is obtained by adding the density-effect correction:

$$\sigma_{\rm Bethe}^{(1)} = \frac{2\pi Z_1^2 e^4}{m_e v^2}\,2Z\left[\ln\left(\frac{2m_e v^2}{I}\right)+\ln\gamma^2-\beta^2+\frac{1}{2}f(\gamma)-\frac{C(\gamma)}{Z}-\frac{1}{2}\delta_F\right]. \tag{61}$$

Because the density-effect correction is significant only for projectiles with high energies (see Fig. 7 below), the value obtained from the formula (59) can also be used when the energy of the projectile is low or moderate.

V. THE BLOCH AND LINDHARD-SØRENSEN CORRECTIONS

As mentioned above, the Bohr stopping-power formula, Eq. (29),

$$S_{\rm Bohr} = \frac{4\pi Z_1^2 e^4}{m_e v^2}\,\mathcal{N}Z\left[\ln\left(\frac{2\exp(-g)\,m_e v^3}{|Z_1|\,e^2\,\overline{\omega}}\right)+\ln\gamma^2-\beta^2\right], \tag{62}$$

is expected to be valid when

$$|\eta| = \frac{|Z_1|e^2}{\hbar v} = \frac{|Z_1|\alpha}{\beta}\gg 1. \tag{63}$$

On the other hand, the Bethe stopping-power formula (40), neglecting the term $f(\gamma)$ that is negligible for heavy projectiles,

$$S_{\rm Bethe} = \frac{4\pi Z_1^2 e^4}{m_e v^2}\,\mathcal{N}Z\left[\ln\left(\frac{2m_e v^2}{I}\right)+\ln\gamma^2-\beta^2\right], \tag{64}$$

is the result from the PWBA, a first-order perturbation calculation, or from the equivalent semiclassical dielectric formalism, which are expected to be valid when [6]

$$Z\alpha\ll\beta. \tag{65}$$

Identifying Bohr's oscillator strength density with the OOS,

$$\frac{df(\omega)}{d\omega} = \hbar\,\frac{df(W)}{dW}, \tag{66}$$

we see that the average binding energy $\hbar\overline{\omega}$ of the classical oscillators [Eq. (28)] and the mean excitation energy I [Eq. (41)] coincide. Then the Bohr and Bethe formulas are seen to differ only in their logarithmic terms:

$$L_{\rm Bohr} = \ln\left(\frac{2\exp(-g)\,m_e v^3\hbar}{|Z_1|\,e^2\,I}\right), \tag{67a}$$

$$L_{\rm Bethe} = \ln\left(\frac{2m_e v^2}{I}\right). \tag{67b}$$

The difference

$$L_{\rm Bohr}-L_{\rm Bethe} = \ln\left(\frac{\exp(-g)}{|\eta|}\right) \tag{68}$$

is determined by the Sommerfeld parameter η and the Euler constant. The relativistic terms, $\ln\gamma^2-\beta^2$, in Eqs. (62) and (64), which have equal contributions from close collisions and distant interactions, vanish in a nonrelativistic approach.

Bloch [14] noticed that the classical nonrelativistic result is more accurate than the perturbative quantum calculation when $\eta^2 \gg 1$, and he derived a correction to the Bethe formula that practically reproduces Bohr's formula when $\eta^2 \gg 1$ and is negligible for small values of η^2. The following derivation of the nonrelativistic Bloch correction is due to Lindhard and Sørensen [15].

If we adhere to the classical view, in which all energy transfers are assumed to be caused by collisions with electrons, and assume that the scattering angle θ in the c.m. frame and the energy transfer W are related by Eq. (14), $W(b) = W_{\max}\,\sin^2[\theta(b)/2]$, the stopping power can be calculated as

$$S_{\rm cl} = \mathcal{N}Z\int W(b)\,2\pi b\,db = \mathcal{N}Z\,W_{\max}\int_0^{b_{\rm ad}} \sin^2[\theta(b)/2]\,2\pi b\,db, \tag{69}$$

where $W_{\max} = 2\beta^2\gamma^2 m_{\rm e}c^2$ is the maximum energy transfer in a collision. Noticing that the classical DCS can be expressed as

$$\frac{d\sigma}{d\Omega} = \frac{2\pi b\,db}{d\Omega} \tag{70}$$

and recalling the definition of the transport cross section (in the c.m. frame, identified here with the reference frame of the projectile),

$$\sigma_{\rm tr} = \int (1-\cos\theta)\,\frac{d\sigma}{d\Omega}\,d\Omega = 4\pi\int_0^{\infty} \sin^2[\theta(b)/2]\,b\,db, \tag{71}$$

we see that the integral in Eq. (69) represents the contribution to the transport cross section of collisions with impact parameters up to the adiabatic cutoff $b_{\rm ad}$. It is then natural to introduce the quantity

$$\sigma_{\rm tr}^{\rm cl}(b_{\rm ad}) \equiv 4\pi\int_0^{b_{\rm ad}} \sin^2[(\theta(b)/2]\,b\,db. \tag{72}$$

In order to put into evidence the relationship with the quantum description of the collision process, we replace the impact parameter b with the angular momentum $\ell\hbar = \gamma\beta m_{\rm e}c\,b$ of the electron in the frame of the projectile, and write

$$\sigma_{\rm tr}^{\rm cl}(\ell_{\rm ad}) = \frac{4\pi}{m_{\rm e}^2v^2}\int_0^{\ell_{\rm ad}} \sin^2[(\theta(\ell)/2]\,\ell\,d\ell \tag{73}$$

with $\ell_{\rm ad} = \gamma\beta m_{\rm e}c\,b_{\rm ad}/\hbar$ and

$$\sin^2[\theta(\ell)/2] = \frac{(Z_1e^2/\beta^2\gamma m_{\rm e}c^2)^2}{(\ell\hbar/\beta\gamma m_{\rm e}c)^2 + (Z_1e^2/\beta^2\gamma m_{\rm e}c^2)^2} = \frac{\eta^2}{\ell^2+\eta^2}. \tag{74}$$

We thus have

$$\sigma_{\rm tr}^{\rm cl}(\ell_{\rm ad}) = \frac{4\pi Z_1^2e^4}{m_{\rm e}^2v^4}\int_0^{\ell_{\rm ad}} \frac{\ell}{\ell^2+\eta^2}\,d\ell, \tag{75}$$

and we can express the classical stopping power as

$$S_{\rm cl} = \mathcal{N}Z\,\frac{W_{\max}}{2}\,\sigma_{\rm tr}^{\rm cl}(\ell_{\rm ad}) = \frac{4\pi Z_1^2e^4}{m_{\rm e}v^2}\,\mathcal{N}Z\,L_{\rm tr}^{\rm cl} \tag{76}$$

with

$$L_{\rm tr}^{\rm cl} = \int_0^{\ell_{\rm ad}} \frac{\ell}{\ell^2+\eta^2}\,d\ell = \frac{1}{2}\,\ln\left(\frac{\ell_{\rm ad}^2+\eta^2}{\eta^2}\right) \simeq \ln\left(\frac{\ell_{\rm ad}}{\eta}\right). \tag{77}$$

Upon comparison with the Bohr logarithm, Eq. (67a), we conclude that the classical-collision approach yields the correct result if the adiabatic cutoff $\ell_{\rm ad}$ is taken to be

$$\ell_{\rm ad} = \frac{2\,\exp(-g)\,m_{\rm e}v^2}{I}. \tag{78}$$

Lindhard and Sørensen [15] considered the analogous calculation of the stopping power based on the transport cross section obtained from the exact quantum description of (nonrelativistic) Coulomb scattering. The transport cross section for Coulomb scattering can be written as [35]

$$\sigma_{\rm tr}^{\rm qu} = \frac{4\pi\,\hbar^2}{m_{\rm e}^2v^2}\sum_{\ell=0}^{\infty}(\ell+1)\,\sin^2(\Delta_\ell - \Delta_{\ell+1}) \tag{79}$$

with the Coulomb phase shifts

$$\Delta_\ell = \arg\Gamma(\ell+1-i\eta). \tag{80}$$

The property

$$\Delta_{\ell+1} = \Delta_\ell + \arctan(-\eta/\ell) \tag{81}$$

implies that

$$\sin^2(\Delta_\ell - \Delta_{\ell+1}) = \frac{\eta^2}{(\ell+1)^2+\eta^2} \tag{82}$$

and, consequently,

$$\sigma_{\rm tr}^{\rm qu} = \frac{4\pi\,\hbar^2}{m_{\rm e}^2v^2}\,\eta^2\sum_{\ell=0}^{\infty}\frac{\ell+1}{(\ell+1)^2+\eta^2} = \frac{4\pi Z_1^2e^4}{m_{\rm e}^2v^4}\sum_{\ell=0}^{\infty}\frac{\ell+1}{(\ell+1)^2+\eta^2}. \tag{83}$$

Comparison with Eq. (75) shows that the quantity

$$L_{\rm tr}^{\rm qu} \equiv \sum_{\ell=0}^{\infty}\frac{\ell+1}{(\ell+1)^2+\eta^2} \tag{84}$$

is analogous to the classical logarithm $L_{\rm tr}^{\rm cl}$, Eq. (77).

Since the Bethe theory is based on a perturbative approach, which is valid for $\eta \ll 1$, we can disregard η^2 in expression (84) and write

$$L_{\rm tr}^{\rm pert} \equiv \sum_{\ell=0}^{\ell'_{\rm ad}}\frac{1}{\ell+1} \simeq \int_1^{\ell'_{\rm ad}}\frac{d\ell}{\ell} = \ln(\ell'_{\rm ad}). \tag{85}$$

The corresponding adiabatic cutoff, $\ell'_{\rm ad}$, is now determined by identifying the quantity (85) with the Bethe logarithm, Eq. (67b). The desired correction is obtained as the difference

$$Z_1^2L_2^{\rm NR} \equiv L_{\rm tr}^{\rm qu} - L_{\rm tr}^{\rm pert} = \sum_{\ell=0}^{\infty}\frac{\ell+1}{(\ell+1)^2+\eta^2} - \sum_{\ell=0}^{\ell'_{\rm ad}}\frac{1}{\ell+1}. \tag{86}$$

Provided η is not too large (i.e., for projectiles with moderate and high speeds), the difference of the unrestricted summations converges rapidly, and we introduce a negligible error by setting

$$Z_1^2 L_2^{\rm NR} = \sum_{\ell=0}^{\infty}\left(\frac{\ell+1}{(\ell+1)^2+\eta^2}-\frac{1}{\ell+1}\right) = -\eta^2\sum_{n=1}^{\infty}\frac{1}{n(n^2+\eta^2)}. \tag{87}$$

This is the Bloch nonrelativistic correction to the Bethe stopping logarithm. The corrected formula

$$S_{\text{Bethe-Bloch}} = \frac{4\pi Z_1^2 e^4}{m_{\rm e}v^2}\mathcal{N}Z\left[\ln\left(\frac{2m_{\rm e}v^2}{I}\right) + \ln\gamma^2-\beta^2+Z_1^2L_2^{\rm NR}\right] \tag{88}$$

is known as the *Bethe-Bloch formula*.

Lindhard and Sørensen [15] extended the nonrelativistic calculation of the Bloch correction to account for relativistic effects. They replaced the nonrelativistic transport cross section (71) with its relativistic generalization expressed in terms of the Dirac–Coulomb phase shifts instead of the Schrödinger-Coulomb phase shifts, which amounts to using the correct relativistic theory of elastic collisions of electrons with pointlike charged projectiles. The relativistic form of the Bloch correction was derived as the difference between the exact [24] transport cross section and its perturbative expansion. This procedure is justified only for low and intermediate energies, say up to $E \approx 10M_1c^2$. At higher energies, the finite size of the charge distribution of the projectile becomes relevant, and one should modify the theory by replacing the Dirac-Coulomb phase shifts with the corresponding phase shifts for scattering of electrons by the projectile's finite-size charge distribution. While the Dirac-Coulomb phase shifts admit an analytical expression, the relativistic phase shifts for scattering of electrons by other potentials have to be calculated numerically.

The stopping-power formula with the Lindhard-Sørensen correction reads

$$S = \frac{4\pi Z_1^2 e^4}{m_{\rm e}v^2}\mathcal{N}Z\left[\ln\left(\frac{2m_{\rm e}v^2}{I}\right) + \ln\gamma^2-\beta^2+\Delta L^{\rm LS}\right]. \tag{89}$$

We have performed numerical calculations of the Lindhard-Sørensen relativistic correction $\Delta L^{\rm LS}$ for projectiles of charge $Z_1 e$ by using the RADIAL subroutines of Salvat and Fernández-Varea [31], for both pointlike and finite-size spherical projectiles. The results for pointlike projectiles with small charges ($|Z_1| \leqslant 2$) and energies less than $10^2 M_1c^2$ are closely approximated by the following analytical expression:

$$\Delta L^{\rm LS}_{\rm point} = \left(\frac{1+A}{1+1.92\,(\gamma-1)^{1.41}}-A\right)Z_1^2L_2^{\rm NR}, \tag{90}$$

where $\gamma-1 = E/(M_1c^2)$, and $A = 180.20$ for $Z_1 = +1$ (protons, deuterons, tritons, and antimuons), $A = -178.34$ for $Z_1 = -1$ (antiprotons and muons), $A = 90.59$ for $Z_1 = +2$ (alphas), and $A = -88.73$ for $Z_1 = -2$. Values from this empirical formula are compared with numerical results calculated for pointlike projectiles with $Z_1 = \pm1$ and ±2 in Fig. 1, the absolute differences being normally less than about 5×10^{-4}.

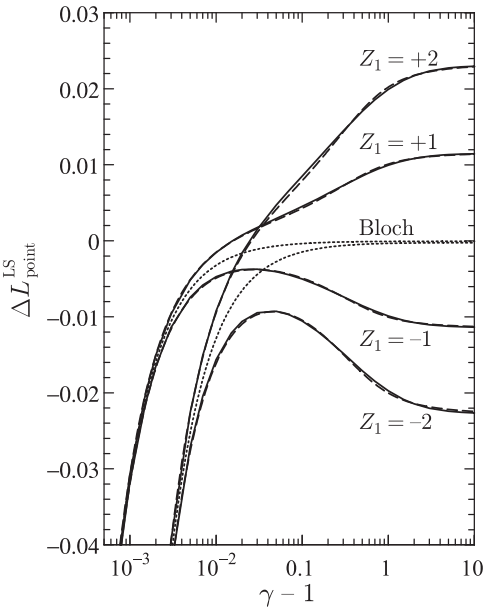

FIG. 1. Lindhard-Sørensen correction for pointlike projectiles with the indicated charge numbers calculated numerically from the Dirac-Coulomb phase shifts (solid curves) and values obtained from the empirical formula (90) (dashed curves). The dotted curves represent the nonrelativistic Bloch correction, Eq. (87), which is proportional to Z_1^2.

Although the correction (90) reduces to the Bloch form, $Z_1^2L_2^{\rm NR}$, for slow projectiles, it also accounts for part of the Z_1^3 and higher-order relativistic corrections. As noted by Lindhard and Sørensen [15], the angular momenta that give sizable contributions to the correction $\Delta L^{\rm LS}$ correspond to impact parameters much smaller than the atomic radii. Therefore, in the following we consider that the Lindhard-Sørensen correction effectively accounts for the Barkas or Z_1^3 correction for close collisions.

VI. THE BARKAS CORRECTION

The Bethe and Bethe-Bloch formulas are even in Z_1 and, consequently, they predict the same stopping power for particles and their antiparticles. However, there is experimental evidence of appreciable differences between the stopping powers for particles with the same masses and opposite charges. The origin of these differences is called the Barkas effect, which introduces a correction term proportional to Z_1^3 in the Bethe formula. In principle, the part of the Barkas effect arising from close collisions is already accounted for by the Lindhard-Sørensen correction. In the following we describe the relativistic calculation of the Barkas-effect correction for distant interactions by Jackson and McCarthy [17], which parallels a nonrelativistic formulation by Ashley *et al.* [16].

In the derivation of Bohr's stopping-power formula, distant interactions were described by assuming that the electric field of the projectile was constant within the volume swept by each bound target electron. Ashley *et al.* [16] went a step further and considered the variation of the electric field with the position of the oscillating electron to first order. The calculation of Ashley *et al.*, extended to the relativistic domain by Jackson and McCarthy [17], gives the following expression for the energy transferred to an oscillator having the binding frequency ω and placed at a distance b from the trajectory of the projectile:

$$W(b,\omega) = \frac{2Z_1^2e^4}{m_e v^2}\frac{1}{b^2}\left[\xi^2K_1^2(\xi)+\frac{1}{\gamma^2}\xi^2K_0^2(\xi)\right]+\frac{2Z_1^3e^6}{m_e^2v^3}\times\frac{1}{b^4\omega_j}\left[-\xi K_1(\xi)G_1(\xi)+\frac{1}{\gamma^2}\xi K_0(\xi)G_0(\xi)\right], \tag{91}$$

where $\xi = \omega b/(\gamma v)$,

$$G_1(\xi) = \int_{-\infty}^{\infty} dx\,\frac{\cos(\xi x)}{(1+x^2)^{5/2}} \times[(x^2-2)F_1(\xi,x) - 3x\,F_2(\xi,x)], \tag{92a}$$

and

$$G_0(\xi) = \int_{-\infty}^{\infty} dx\,\frac{\sin(\xi x)}{(1+x^2)^{5/2}} \times[3x\,F_1(\xi,x) - (1-2x^2)\,F_2(\xi,x)], \tag{92b}$$

with

$$F_1(\xi,x) = \int_{-\infty}^{y}\frac{\sin[\xi(x-y)]}{(1+y^2)^{3/2}}\,dy \tag{93a}$$

and

$$F_2(\xi,y) = \int_{-\infty}^{x}\frac{y\,\sin[\xi(x-y)]}{(1+y^2)^{3/2}}\,dy. \tag{93b}$$

The first term in expression (91) is the known zeroth-order result, given by Eq. (21), and the second term represents the Barkas-effect correction.

The classical stopping power of distant oscillators, with impact parameters larger than the cutoff value a, is

$$S^{\rm B}_{{\rm cl},b>a} = 2\pi\mathcal{N}\int_0^{\infty}d\omega\,\frac{df(\omega)}{d\omega}\int_a^{\infty}W(b,\omega)\,b\,db = S_{{\rm cl},b>a} + \Delta S_{{\rm cl},b>a}. \tag{94}$$

The contribution of the zeroth-order term is given by Eq. (25), and that of the Z_1^3 term is

$$\Delta S_{{\rm cl},b>a} = 2\pi\mathcal{N}\int_0^{\infty}d\omega\,\frac{df(\omega)}{d\omega}\int_a^{\infty}db\,b\left\{\frac{2Z_1^3e^6}{m_e^2v^3}\times\frac{1}{b^4\omega}\left[-\xi K_1(\xi)G_1(\xi)+\frac{1}{\gamma^2}\xi K_0(\xi)G_0(\xi)\right]\right\} = \frac{4\pi\,Z_1^3e^6}{\gamma^2m_e^2v^5}\mathcal{N}\int_0^{\infty}d\omega\,\frac{df(\omega)}{d\omega}\,\omega\times\left[I_1(\xi_a)+\frac{1}{\gamma^2}I_2(\xi_a)\right] \tag{95}$$

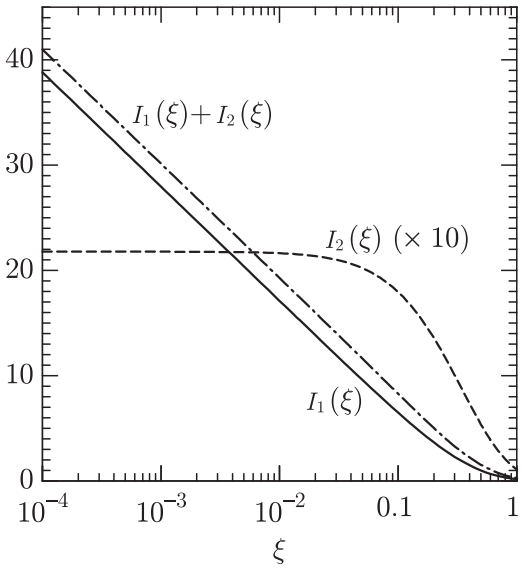

FIG. 2. Calculated $I_1(\xi)$ and $I_2(\xi)$ functions, Eqs. (96), as functions of the dimensionless variable $\xi = \omega a/\gamma v$.

with

$$I_1(\xi_a) = -\int_{\xi_a}^{\infty}\frac{1}{\xi^2}K_1(\xi)\,G_1(\xi)\,d\xi \tag{96a}$$

and

$$I_2(\xi_a) = \int_{\xi_a}^{\infty}\frac{1}{\xi^2}K_0(\xi)\,G_0(\xi)\,d\xi, \tag{96b}$$

where $\xi_a = \omega a/(\gamma v)$.

Because we have been unable to find published numerical tables, we have computed the functions $I_1(\xi_a)$ and $I_2(\xi_a)$ numerically as follows. First, the functions $G_1(\xi)$ and $G_0(\xi)$ were evaluated from their expressions (92) by using an adaptive 20-point Gauss-Legendre quadrature method, for a suitably spaced grid of ξ values. Then the integrals $I_1(\xi_a)$ and $I_2(\xi_a)$ were computed from Eqs. (96), with $G_1(\xi)$ and $G_0(\xi)$ replaced with their interpolating cubic splines, by using the adaptive Gauss-Legendre method. The numerical results are generally accurate to four or five digits, and they are displayed in Fig. 2 for $\xi \leqslant 1$. Finally, to facilitate numerical calculations, the tabulated functions have been fitted by analytical expressions that approximate the numerical results with an accuracy better than 0.1% for ξ from 0 to ≈15.

The Barkas correction to the stopping power of distant oscillators is

$$\Delta S_{{\rm cl},b>a} = \frac{4\pi\,Z_1^2e^4}{m_e v^2}\mathcal{N}Z\,\Delta L^{\rm B}(a) \tag{97}$$

where $\Delta L^{\rm B}(a)$, the correction to the stopping logarithm, expressed in terms of the energy loss W, is

$$\Delta L^{\rm B}(a) = \frac{Z_1\alpha}{\gamma^2\beta^3m_ec^2}\frac{1}{Z}\int_0^{W_{\rm max}}dW\,\frac{df(W)}{dW}\times W\left[I_1(\xi)+\frac{1}{\gamma^2}I_2(\xi)\right], \tag{98}$$

with $\xi = Wa/(\gamma v\hbar)$. Notice that the upper limit of the integral has been replaced with $W_{\max}$, because larger energy transfers are not permitted.

The derivation of the Bohr formula, Eq. (29), shows that the dependence on the cutoff impact parameter a is removed when adding the contributions to the stopping power of close collisions and distant interactions. Unfortunately, the Barkas correction, Eq. (98), does depend on a, which thus becomes an essential parameter of the theory that can only be estimated from qualitative arguments [17,36]. Lindhard [36], based on considerations of stopping by an electron gas, proposed using a value of the order of the impact parameter that corresponds to an angular momentum equal to $\hbar$, namely,

$$a = \exp(-g)\,\frac{\hbar}{m_e v}, \tag{99}$$

where g is the Euler constant, and $\exp(-g) = 0.5616$. Notice that this a value is independent of the energy transfer. In the case of protons in aluminium, Ashley [37] found that the calculated correction to the stopping power with Lindhard's a value agrees reasonably with experimental results. Because of the approximate character of the Barkas correction, it is expedient to allow a certain flexibility and define the cutoff impact parameter as

$$a = C_B \exp(-g)\,\frac{\hbar}{m_e v}, \tag{100}$$

where C_B is a dimensionless constant, of the order of unity, to be determined empirically. A systematic comparison with results from measurements of the stopping power of elemental materials for protons and alphas in the IAEA database indicates that a value of C_B between 1 and 10 (increasing roughly with Z) yields stopping powers in reasonable agreement with the experiments.

VII. THE CORRECTED BETHE FORMULA

Adding to the formula (43) the density-effect correction [Eq. (59)], the Lindhard-Sørensen correction [approximated by the parametrization (90)] and the Barkas correction [Eq. (98)], we obtain the corrected Bethe formula for the stopping power:

$$S = \frac{4\pi Z_1^2 e^4}{m_e v^2}\,\mathcal{N}Z\left[\ln\left(\frac{2m_e v^2}{I}\right) + \ln\gamma^2 - \beta^2 + \frac{1}{2}f(\gamma) - \frac{C(\gamma)}{Z} - \frac{1}{2}\delta_F + \Delta L^{LS} + \Delta L^{B}(a)\right]. \tag{101}$$

The mean excitation energy I, the density-effect, and the Barkas corrections are determined by the OOS of the material. The formula (101), with the appropriate I value and with these corrections evaluated from a suitable OOS, is considered to provide realistic values of the stopping power of elemental and compound materials for fast charged projectiles. In the past, however, due to the lack of precise knowledge about the shell correction, the term C/Z had to be obtained from approximations or derived from a fit to experimental data (see, e.g., Refs. [38,39]).

Recent calculations of inelastic collisions of charged projectiles with free atoms by Salvat *et al.* [8] have disclosed a limitation of the Bethe formula, which originates from the fact that the relativistic GOSs do not obey the Bethe sum rule [40–43], and the functions

$$S_0(Q) \equiv \int_0^\infty \frac{df(Q,W)}{dW}\,dW \tag{102}$$

and

$$T_0(Q) \equiv \int_0^\infty \frac{dg(Q,W)}{dW}\,dW \tag{103}$$

vary with Q. In the optical ($Q = 0$) limit,

$$S_0(0) = T_0(0) = Z[1 - \Delta], \tag{104}$$

where Δ, the relativistic departure from the dipole sum rule, is negligible for hydrogen ($Z = 1$) and increases nearly monotonically with Z being $\approx$0.025 for einsteinium ($Z = 99$). For sufficiently large Q, where the GOSs reduce to the Bethe ridge, both $S_0(Q)$ and $T_0(Q)$ tend to Z, i.e., the Bethe sum rule is fulfilled. Although the relativistic departure is relatively small, it adds an extra term to the stopping-power formula and, more important, it leads to a definition of the mean excitation energy different from the conventional one, Eq. (41).

Salvat *et al.* [8] have performed systematic calculations of the total, stopping, and energy-straggling cross section, for all atoms (Z = 1–99) and projectile protons with kinetic energies from 1 keV up to 100 GeV by using the DHFS model. They also derived asymptotic formulas that approximate these calculated cross sections when the kinetic energy of the projectile is sufficiently high. The asymptotic formula for the stopping cross section reads

$$\sigma_{as}^{(1)} = \frac{2\pi Z_1^2 e^4}{m_e v^2}\left\{[S_0 + Z][\ln(\beta^2\gamma^2) - \beta^2] + 2\,S_0 \ln\left(\frac{2m_e c^2}{I_0}\right) + D_0 + Z\,f(\gamma)\right\} \tag{105}$$

where

$$S_0 = S_0(0) = \int_0^\infty \frac{df(W)}{dW}\,dW \tag{106}$$

is the dipole sum,

$$\ln I_0 = \frac{1}{S_0}\int_0^\infty \ln W\,\frac{df(W)}{dW}\,dW, \tag{107}$$

$$f(\gamma) = \ln(R) + \left(\frac{m_e}{M}\,\frac{\gamma^2 - 1}{\gamma}\,R\right)^2, \tag{108}$$

and the dimensionless parameter D_0 is defined as an integral of the longitudinal GOS. Figure 3 shows the values of the parameter S_0 obtained from the numerical OOSs of neutral atoms computed with the DHFS potential. The value of D_0 obtained from the corresponding longitudinal GOS is $\approx 5 \times 10^{-4}\,Z^2$.

It is interesting to compare the formula (105) with the conventional Bethe formula, Eq. (40) with the *mean excitation energy* I defined by Eq. (41), for the stopping cross section of free atoms [23,38,39]. The derivation of the Bethe formula (see, e.g., Ref. [5]) makes explicit use of the Bethe sum rule [$S_0(Q) = Z$], which is assumed to hold for any Q. Consequently, the formula (40) is strictly valid only for light elements, for which relativistic deviations from the sum

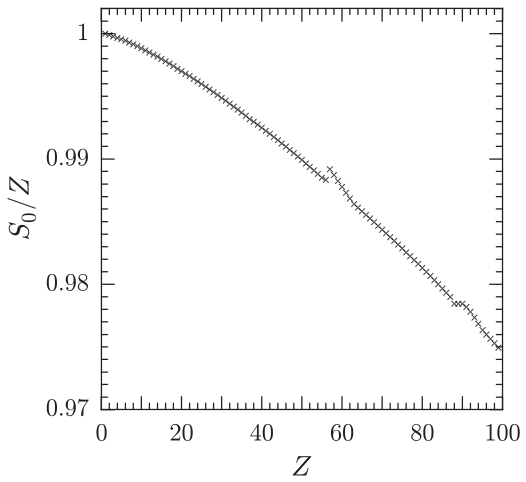

FIG. 3. Values of the dipole sum S_0 calculated from the numerical OOSs of neutral atoms (DHFS model). For the sake of clarity, the ratio S_0/Z is plotted vs Z. From Salvat *et al.* [8].

rule are small and do not modify appreciably the calculated stopping cross sections.

The asymptotic formula (105) can be expressed similarly to the Bethe formula (40):

$$\sigma_{\rm as}^{(1)} = \frac{2\pi Z_1^2 e^4}{m_e v^2}\,2Z\left\{\ln\left(\frac{2m_e v^2}{I_0'}\right) + \ln\gamma^2 - \beta^2 + \frac{1}{2}f(\gamma) + \frac{S_0 - Z}{2Z}[\ln(\beta^2\gamma^2) - \beta^2]\right\}, \tag{109}$$

where we have grouped the energy-independent terms by introducing the "modified" mean excitation energy I_0' defined by

$$\ln\left(\frac{2m_e c^2}{I_0'}\right) = \frac{S_0}{Z}\ln\left(\frac{2m_e c^2}{I_0}\right) + \frac{D_0}{2Z}. \tag{110}$$

Evidently, Eq. (109) reduces to the Bethe formula when $S_0 = Z$ (the OOS satisfies the dipole sum rule) and $D_0 = 0$. Under these circumstances, we also have $I_0' = I_0 = I$. Although the relativistic departure from the Bethe sum rule is small in magnitude, about 2.5% for einsteinium ($Z = 99$), the relative difference between the calculated I_0 and I_0' values is relevant, of the order of 15% for $Z = 99$ [8].

Salvat *et al.* [8] also determined the shell correction, $C(\gamma)/Z$, for atoms from the difference between the stopping cross section calculated numerically (by integration of the energy-loss DCS obtained from GOSs computed with the DHFS potential) and the asymptotic formula (109). As mentioned in the Introduction, since the main contributions to the shell correction originate from inner electron subshells, which are assumed to be described accurately by the DHFS model, the shell correction calculated for free DHFS atoms is expected to be applicable also to dense materials and compounds.

Hence, at least for elemental materials, one can account for the relativistic departure from the Bethe sum rule by adopting the asymptotic formula (109) for the stopping cross section of the unpolarizable material. Addition of the shell, density-effect, Lindhard-Sørensen, and Barkas corrections yields the *corrected Bethe formula for the stopping power*:

$$S = \frac{4\pi Z_1^2 e^4}{m_e v^2}\mathcal{N}Z\left\{\ln\left(\frac{2m_e v^2}{I_0'}\right) + \ln\gamma^2 - \beta^2 + \frac{1}{2}f(\gamma) + \frac{S_0 - Z}{2Z}[\ln(\beta^2\gamma^2) - \beta^2] - \frac{C(\gamma)}{Z} - \frac{1}{2}\delta_{\rm F} + \Delta L^{\rm LS} + \Delta L^{\rm B}(a)\right\}. \tag{111}$$

Naturally, if the "modified" mean excitation energy I_0' is considered as an adjustable parameter, and we define the modified shell correction

$$\frac{C_0'(\gamma)}{Z} = \frac{Z - S_0}{2Z}[\ln(\beta^2\gamma^2) - \beta^2] + \frac{C(\gamma)}{Z}, \tag{112}$$

the formula (111) takes the same form as the corrected Bethe formula (101).

VIII. OPTICAL OSCILLATOR STRENGTHS OF MATERIALS

As indicated above, the OOS,

$$F(W) \equiv \frac{df(W)}{dW} = W\,\frac{2Z}{\pi(\hbar\Omega_{\rm p})^2}\,{\rm Im}\left(\frac{-1}{\epsilon(W)}\right), \tag{113}$$

determines the mean excitation energy I, the density-effect correction $\delta_{\rm F}$, and the Barkas correction $\Delta L^{\rm B}$. The OOS is also the basis of the so-called optical-data models of the GOS that are used for computing reliable interaction data for electrons and positrons (see Refs. [44,45] and references therein) and in Monte Carlo simulations [46]. These models start from an empirical OOS to build the longitudinal GOS (or the dielectric function) for $Q > 0$ by using an "extension" algorithm, usually based on the free-electron gas theory [45,47–49].

In principle, the most reliable OOSs of materials are obtained from experimental information on optical constants. The required information can be inferred from measurements with monochromatized synchrotron radiation (see, e.g., Ref. [50]). The main source of measured optical data is the *Handbook of Optical Constants of Solids* [51–53], which includes tables of optical constants for a number of metals, semiconductors, and insulators. These tables contain the refractive index $n(W)$ and the extinction coefficient $\kappa(W)$ measured with different methods, frequently by various groups and with various degrees of accuracy. They cover a range of excitation energies $W = \hbar\omega$ from about 10^{-3} eV up to an upper energy that depends on the material, typically about 100 eV. The real and imaginary parts of the optical dielectric function, $\epsilon(W) = \epsilon_1(W) + i\,\epsilon_2(W)$, are

$$\epsilon_1(W) = n^2(W) - \kappa^2(W), \tag{114a}$$

$$\epsilon_2(W) = 2\,n(W)\,\kappa(W), \tag{114b}$$

and the OOS is obtained from Eq. (113):

$$\frac{df(W)}{dW} = W\,\frac{2Z}{\pi(\hbar\Omega_{\rm p})^2}\,\frac{\epsilon_2(W)}{\epsilon_1^2(W) + \epsilon_2^2(W)}. \tag{115}$$

Alternatively, empirical OOSs of solids can be derived from electron energy-loss measurements (see, e.g., Ref. [54]). For solids for which experimental information is not available,

approximate OOSs could be obtained from density-functional theory calculations [55]. The tables of photon interaction coefficients of Henke *et al.* [56,57], which were derived from a compilation of experimental data and calculations, cover the energy range from 30 eV to 30 keV for the elements with $Z = 1$ to 92. Because empirical information is available only for limited energy ranges, it must be complemented with atomic OOSs calculated from a realistic model.

It is worth mentioning that composite OOSs derived from measured optical data are affected by experimental uncertainties. As a consequence, the intermediate dielectric function may not comply with the principle of causality [11,58], which requires that the real and imaginary parts of the optical energy-loss function $\epsilon^{-1}(W)$ satisfy the Kramers–Kronig relations,

$$\mathrm{Re}\left(\frac{1}{\epsilon(W)}\right) = 1 - \frac{2}{\pi}\mathcal{P}\int_0^\infty \frac{W'}{W'^2 - W^2}\,\mathrm{Im}\left(\frac{-1}{\epsilon(W)}\right)dW' \tag{116a}$$

and

$$\mathrm{Im}\left(\frac{-1}{\epsilon(W)}\right) = \frac{2W}{\pi}\mathcal{P}\int_0^\infty \frac{1}{W'^2 - W^2} \times\left[\mathrm{Re}\left(\frac{1}{\epsilon(W)}\right) - 1\right]dW', \tag{116b}$$

where $\mathcal{P}$ indicates the principal value of the integral. When these relations are not approximately satisfied, the OOS obtained from the input optical data is not reliable.

As the OOS of a specific material may not be available, simple approximate models are frequently employed in calculations. One of these is the statistical model of Lindhard and Scharff [59], which is used, e.g., by Ashley *et al.* [16], by Jackson and McCarthy [17], and in the ICRU Report 49 [39]. The basis of the model is the local-plasma approximation (LPA) which applies to a system of bound electrons characterized by the electron density $\rho(\mathbf{r})$ (number of electrons per unit volume); it is assumed that electrons at $\mathbf{r}$ react to external electromagnetic fields in the same way as if they were in a homogeneous electron gas of density $\rho(\mathbf{r})$. The OOS resulting from the LPA can be expressed as [60]

$$F_{\mathrm{LPA}}(W) = \int d\mathbf{r}\,\rho(\mathbf{r})\,\delta\{W - \tau\hbar\omega_{\mathrm{p}}[\rho(\mathbf{r})]\} \tag{117}$$

where

$$\hbar\omega_{\mathrm{p}}(\rho) = \hbar\sqrt{4\pi\rho e^2/m_{\mathrm{e}}} \tag{118}$$

is the plasma resonance energy of an electron gas with density ρ. The parameter τ, which defines a rescaling of the energy axis, is introduced empirically with the purpose of ensuring that the OOS (118) yields, through the definition (41), the empirical value of the mean excitation energy I. Qualitative considerations [59,61] indicate that the value of τ should be between 1 and 2. The statistical model combines the LPA with the electron density of the Thomas-Fermi atom, which may be approximated as [62]

$$\rho(r) = \frac{Z}{4\pi b^2 r}[3.6\exp(-6\,r/b) + 0.792\exp(-1.2\,r/b) + 0.0315\exp(-0.3\,r/b)], \tag{119}$$

where $b = 0.885\,34 a_0 Z^{-1/3}$ is the Thomas-Fermi radius, and a_0 is the Bohr radius. Although the statistical model is useful to estimate global stopping properties of elemental materials, it is too schematic to be employed for quantitative purposes. It is worth mentioning that a shell-local LPA, applied to electron densities of individual electron shells, yields realistic stopping powers for nonrelativistic ions (see Ref. [63] and references therein).

A convenient approach is to use the OOSs (i.e., the GOS at $Q = 0$) calculated from the DHFS model of the atom, which we have extracted from our database of subshell GOSs [8]. Let $F_i^{\mathrm{ion}}(Z;W)$ denote the calculated OOS for transitions of individual electrons in the ith subshell of the atom to final orbitals with positive energy (ionization). Because the subshell ionization energies U_i obtained from the DHFS potential differ slightly from the experimental ionization energies, the subshell OOS is shifted in energy to the correct (empirical) ionization energies given by Carlson [64]. For the purposes of stopping calculations, excitations to bound atomic levels (a series of discrete resonances with energies below U_i) must be taken into account to ensure that the resulting OOS does preserve the dipole sum. Because the fine details of the excitation spectrum are not important, the contribution of discrete excitations to the OOS has been represented approximately by extending the ionization OOS to excitation energies below the ionization threshold. Explicitly, the OOS of the ith subshell is described as

$$F_i(Z;W) = \begin{cases} F_i^{\mathrm{ion}}(Z;W) & \text{if } U_i \leqslant W, \\ F_i^{\mathrm{ion}}(Z;U_i) & \text{if } U_i' \leqslant W < U_i, \\ 0 & \text{if } W < U_i', \end{cases} \tag{120}$$

with the cutoff energy U_i' such that the product $(U_i - U_i')F_a^{\mathrm{ion}}(Z;U_i)$ equals the sum of OOSs for excitations to discrete levels. For the outmost subshells the cutoff energy so defined may be less than $0.5U_i$; in this case, the recipe (120) is modified by setting $U_i' \simeq 0.5U_i$, and defining the constant OOS in the interval (U_i', U_i) so that the subshell contribution to the dipole sum is preserved.

In the case of a monoatomic gas of the element with atomic number Z, the OOS can be approximated in terms of the subshell OOSs in the database as

$$F_{\mathrm{atom}}(Z;W) = \sum_i F_i(Z;W), \tag{121}$$

where the summation runs over the various electron subshells of the atom in its ground-state configuration. As indicated above, this atomic OOS deviates slightly from the dipole sum rule because of relativistic effects. Since the dipole sum rule is instrumental in the derivation of the Bethe stopping-power formula (40), and the relativistic departure is small, the OOS is renormalized to fulfill that sum rule. In addition, to ensure agreement of stopping powers obtained from the Bethe formula with measurements, we shall rescale the excitation energies so as to reproduce the empirical value of the mean excitation energy I, Eq. (41). That is, we consider the OOS

$$F(Z;W) = a_1 a_2 F_{\mathrm{atom}}(Z;a_2\,W) \tag{122}$$

with the constants a_1 and a_2 determined from the conditions

$$Z = \int_0^\infty F(Z;W)\,dW = a_1 \int_0^\infty F_{\rm atom}(Z;W')\,dW', \quad (123a)$$

where $W' = a_2 W$, and

$$\begin{aligned}\ln I &= \frac{1}{Z}\int_0^\infty \ln W\, F(Z;W)\,dW \\ &= \frac{1}{Z}\,a_1 \int_0^\infty \ln(W'/a_2)\, F_{\rm atom}(Z;W')\,dW' \\ &= -\ln a_2 + \frac{a_1}{Z}\int_0^\infty \ln W'\, F_{\rm atom}(Z;W')\,dW'.\end{aligned} \quad (123b)$$

The recipe given by Eqs. (122) and (123) is not suited for compounds and condensed materials, because the wave functions of electrons in outer subshells are strongly affected by atomic aggregation. In addition, the presence of neighboring atoms modifies the final-state orbitals of the active electron [65]. The contributions from inner subshells with binding energies U_i larger than a certain threshold value $W_{\rm th}$ of the order of 50 eV are relatively insensitive to aggregation and may be approximated by the free-atom form (121). The OOS of electrons in outer subshells with binding energies $U_i < W_{\rm th}$ will be represented as the OOS of a single classical damped oscillator with resonance energy W_r and damping constant Γ. In the case of insulators and semiconductors, an energy gap $W_{\rm g}$ may be introduced. Explicitly, we set

$$\begin{aligned}F_{\rm out}(W) = C_{\rm out}\,&\frac{W\sqrt{W^2 - W_{\rm g}^2}}{\left(W_{\rm r}^2 + W_{\rm g}^2 - W^2\right)^2 + \Gamma^2\left(W^2 - W_{\rm g}^2\right)} \\ &\times \Theta(W - W_{\rm g})\,\Theta(U_{\rm K,max} - W),\end{aligned} \quad (124)$$

where $C_{\rm out}$ is a normalization constant and $\Theta(x)$ is the Heaviside step function (=1 if $x > 0$, and $= 0$ otherwise). The OOS of the oscillator is truncated at the largest binding energy $U_{\rm K,max}$ of the K shells of the elements present to prevent a tail that would dominate over the atomic OOSs at very large Ws. The model OOS is obtained as

$$F(W) = F_{\rm out}(W) + \sum_i F_i(Z;W)\,\Theta(W - W_{\rm th}), \quad (125)$$

where the summation runs over the inner subshells. Notice that the OOSs of inner subshells are truncated at $W_{\rm th}$. The constant $C_{\rm out}$ is determined by requiring that the dipole sum rule is satisfied, i.e.,

$$\begin{aligned}\int_{W_{\rm g}}^{U_{\rm K,max}} F_{\rm out}(W)\,dW &= Z - \int_{W_{\rm th}}^\infty \left(\sum_i F_i(Z;W)\right) dW \\ &= f_{\rm out},\end{aligned} \quad (126)$$

and the resonance energy $W_{\rm r}$ is set equal to the plasma resonance energy of an electron gas with the average density of electrons in outer subshells (including contributions from truncated inner subshells):

$$W_{\rm r} = \hbar\sqrt{4\pi\mathcal{N} f_{\rm out} e^2/m_{\rm e}}. \quad (127)$$

The gap energy $W_{\rm g}$ is defined by the user, possibly guided by experimental information; for conductors, $W_{\rm g} = 0$. Finally the damping constant Γ is fixed by requiring that the OOS yields the empirical I value of the material, as given, e.g., in the ICRU Report 37 [20]. The resulting OOS has a realistic appearance for large energy transfers W, it satisfies the f-sum rule, and it yields the adopted empirical I value.

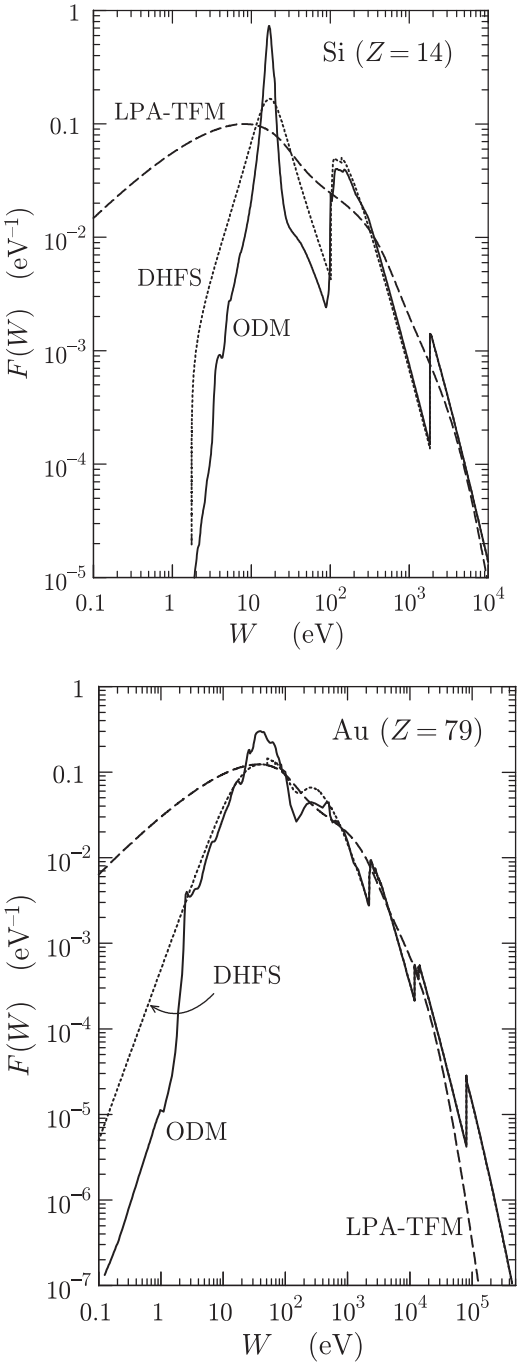

FIG. 4. Optical oscillator strengths of silicon and gold. ODM: solid curves, experimental optical data, complemented with DHFS calculated OOS of inner subshells. DHFS: dotted curves, atomic DHFS model with outer-shell electrons represented by a single oscillator. LPA-TFM: dashed curves, LPA with Thomas-Fermi-Molière density (119).

Figure 4 displays empirical OOSs of solid silicon and gold determined from experimental optical data (as described in

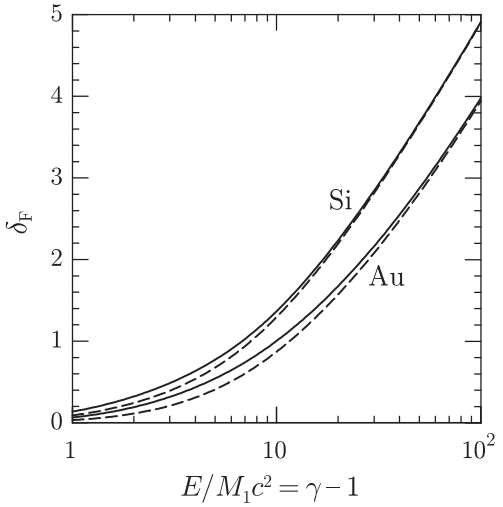

FIG. 5. Density-effect correction δ_F for charged projectiles in solid silicon and gold calculated from the optical-data OOS (solid curves) and from the DHFS-model OOS (dashed curves), as a function of the reduced kinetic energy of the projectile.

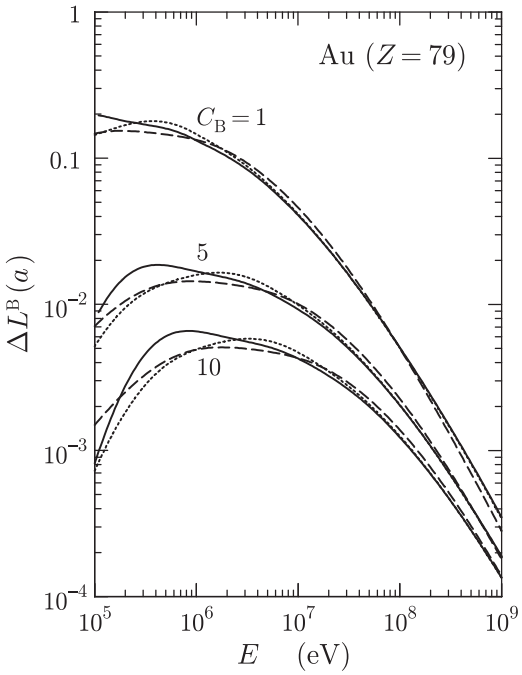

FIG. 6. Barkas correction for protons in gold, calculated from the OOSs displayed in Fig. 4, for the indicated values of the parameter C_B, Eq. (100), as a function of the proton energy. Optical-data OOS, solid curves; LPA OOS, dashed curves; DHFS-model OOS, dotted curves.

Ref. [45]), obtained from the LPA with the Thomas-Fermi-Molière electron density (119), and calculated from the DHFS model [Eq. (125)]. The OOS for both the LPA and the DHFS model were required to reproduce the empirical I values recommended in Ref. [20] ($I_{Si} = 173$ eV, $I_{Au} = 790$ eV); the energy gap for silicon was $W_g = 1.75$ eV. It is worth noticing that, since experimental optical data are available only for energy transfers up to a finite value, they are complemented with DHFS-model values for higher W. The OOSs derived from DHFS-model calculations agree closely with those obtained from optical data, except at low W where the simplicity of the one-oscillator model gets manifest. The OOSs calculated from the LPA are seen to differ markedly from the optical-data OOS, despite the fact that they have been repeatedly used in calculations of the Barkas correction [16,17,39].

As shown in Fig. 5, the density-effect corrections, Eq. (59), calculated from the OOS built with optical data and from the DHFS-model OOS, differ appreciably for projectiles with small and moderate energies, but the difference reduces when the energy of the projectile increases. In practice, these differences have a negligible impact on the resulting stopping power because the density-effect correction is significant only when the energy of the projectile is higher than $\approx M_1c^2$ (see Fig. 7 below).

In order to assess the dependence of the Barkas correction, Eq. (98), on the adopted OOS, $\Delta L^B(a)$ values for protons in gold, calculated from the OOSs shown in Fig. 4 for the indicated values of the parameter C_B, are displayed in Fig. 6 as functions of the kinetic energy E of the projectile. Evidently, the magnitude of the correction decreases when C_B increases. For energies below about 1 MeV, the corrections calculated from the three OOS models differ appreciably because of the rather different shapes of the OOSs. When the energy of the projectile increases, the difference between results from the optical-data and the DHFS-model OOSs decreases and becomes negligible for energies higher than about 10 MeV, quite independently of the atomic number. The LPA and the optical-data OOSs yield similar results for elements with low atomic numbers, although for heavy elements the LPA tends to overestimate the correction in a range of intermediate energies.

The similarity between the empirical OOS built from optical data and the OOS obtained from the DHFS model, combined with their near equivalence in calculations of the Barkas correction for high-energy projectiles, justifies the adoption of the DHFS model as the "default" OOS in practical evaluations. In what follows we shall calculate the density-effect and Barkas corrections from the DHFS-model OOSs, as defined by Eq. (122) or (125), with the empirical value of the mean excitation energy I recommended in the ICRU Report 37 [20].

IX. COMPARISON WITH EXPERIMENTAL DATA

The corrected Bethe formula, Eqs. (111) and (112),

$$S = \frac{4\pi Z_1^2 e^4}{m_e v^2}\mathcal{N}Z\left\{\ln\left(\frac{2m_e v^2}{I_0'}\right) + \ln\gamma^2 - \beta^2 + \frac{1}{2}f(\gamma) - \frac{C_0'(\gamma)}{Z} - \frac{1}{2}\delta_F + \Delta L^{LS} + \Delta L^B(a)\right\}, \quad (128)$$

is expected to provide a consistent theoretical basis for calculating the stopping power of a material for charged projectiles with sufficiently high energies. Assuming that our numerical calculations with the DHFS-model GOSs [8] provide realistic values of the effective shell correction, $C_0'(\gamma)/Z$, and that the density-effect and the Barkas corrections obtained from the adopted (DHFS-model) OOS are accurate, the only

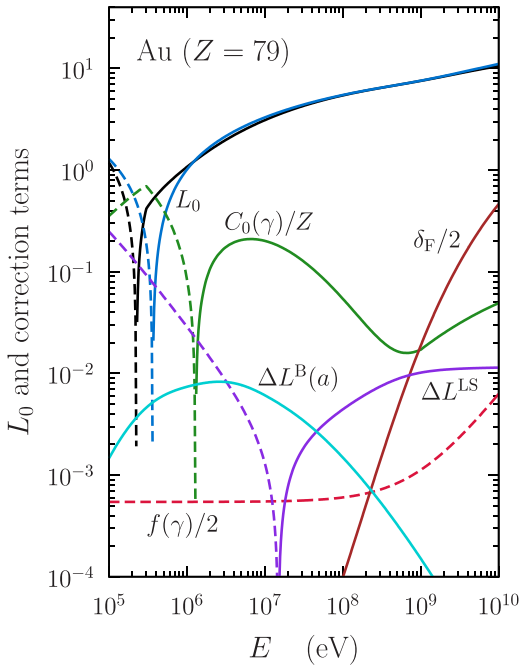

FIG. 7. Bethe logarithmic term L_0, Eq. (129), and correction terms in the corrected Bethe formula for protons in solid gold, calculated from the DHFS-model OOSs shown in Fig. 4, as functions of the kinetic energy of the projectile. The black curve is the sum of terms within the curly braces in Eq. (128). The dashed curves represent negative values.

parameters that remain undefined are the mean excitation energy I_0', which is strongly affected by uncertainties in the OOS, and the cutoff impact parameter a (or, equivalently, C_B), which is not determined by the theory. In principle, these two parameters could be obtained by numerical fitting to available experimental stopping-power data.

Before attempting further evaluations, it is convenient to get a feel of the relative importance of the various terms in the formula (128). The dominant contribution comes from the "logarithmic" term

$$L_0 = \ln\left(\frac{2m_e v^2}{I_0'}\right) + \ln\gamma^2 - \beta^2, \tag{129}$$

which depends on the mean excitation energy I_0'. Figure 7 displays the various terms in the curly braces of Eq. (128), for protons in gold, calculated with $I_0' = 790$ eV, the empirical I value given in the ICRU Report 37 [20], and $C_B = \max\{1, Z/10\}$ (see below). Notice that the shell and the density-effect corrections, considered as functions of the speed of the projectile, are independent of the projectile kind. The shell correction dominates for protons with energy in the interval between about 1 and 100 MeV. The Barkas correction is roughly proportional to (and has the sign of) the particle charge. It is larger for alphas than for protons, by a factor of about 2 at intermediate energies.

In order to elucidate the possibility of determining the parameters I_0' and C_B from experimental data, we consider the IAEA stopping-power database of elemental materials for protons and alpha particles [19]. Initially, we transformed the measured stopping powers S_{exp} by isolating the terms in the corrected Bethe formula (128) that contain the parameters to be fitted. Specifically, we considered the reduced quantity

$$\begin{aligned} S_{red} &\equiv S_{exp}\left(\frac{4\pi Z_1^2 e^4}{m_e v^2}\mathcal{N}Z\right)^{-1} - \left[\ln\left(\frac{2m_e v^2}{I_{ICRU}}\right)\right. \\ &\quad \left. + \ln\gamma^2 - \beta^2 + \frac{1}{2}f(\gamma) - \frac{C_0'(\gamma)}{Z} - \frac{1}{2}\delta_F + \Delta L^{LS}\right] \\ &= \ln\left(\frac{I_{ICRU}}{I_0'}\right) + \Delta L^B(a), \end{aligned} \tag{130}$$

where I_{ICRU} are the I values recommended in the ICRU Report 37 [20], which were determined by combining information from multiple sources and are expected to be fairly realistic. Evidently, varying the value of I_0' amounts to a constant shift of the S_{red} vs E curve; the only dependence of S_{red} on the energy of the projectile is associated to the Barkas correction. The latter is calculated from the formula (98) with the DHFS-model OOS and the cutoff impact parameter given by Eq. (100), by considering the constant C_B as the parameter to be fitted. It should be mentioned that the availability of a supposedly reliable shell correction [8] largely simplifies the fitting process. Previous similar attempts [38,39] faced the problem of lacking information on the shell correction, which was left out of the reduced stopping power, and had to be either included in the fitting process or estimated from the LPA or from hydrogenic models.

It is worth recalling that the Bethe formula is not expected to work for projectiles with low energies, at which the PWBA loses reliability. Indeed, the formula (128) yields negative (i.e., manifestly incorrect) values of the stopping power for low-energy projectiles (see Fig. 7). Guided by a tentative comparison of results from the present calculation scheme with experimental stopping-power data in the IAEA database we concluded that the corrected Bethe formula (128) is valid for energies higher than a cutoff value $E_{cut} \simeq 0.75$ MeV for protons and $\simeq 5$ MeV for alphas, because its predictions seem to depart from the trend of experimental data at lower energies. Consequently, only S_{red} values for energies higher than E_{cut} were used for fitting the parameters I_0' and C_B.

For the few materials for which there are enough stopping-power measurements available at energies higher than E_{cut}, a plot of their reduced values S_{red}, Eq. (130), vs the kinetic energy of the projectile allows assessing the possibility of the fit. Ideally S_{red} should be a continuous function of the projectile's kinetic energy. In practice, however, the experimental data yield a highly scattered cloud of reduced stopping powers, indicating that experimental uncertainties translate into large fluctuations of S_{red} that may invalidate the fit. The situation is illustrated in Fig. 8, that displays the "experimental" S_{red} values for protons in aluminium, copper, silver, and gold, which are the materials for which measured data are more abundant. A similar situation is found for other elements and also for alpha particles. We have determined the parameters I_0' and C_B from a least-squares fit of the function

$$\mathcal{G}(E) = \ln\left(\frac{I_{ICRU}}{I_0'}\right) + \Delta L^B(a) \tag{131}$$

to the S_{red} values corresponding to the measured stopping powers in the IAEA database with energies higher than E_{cut}.

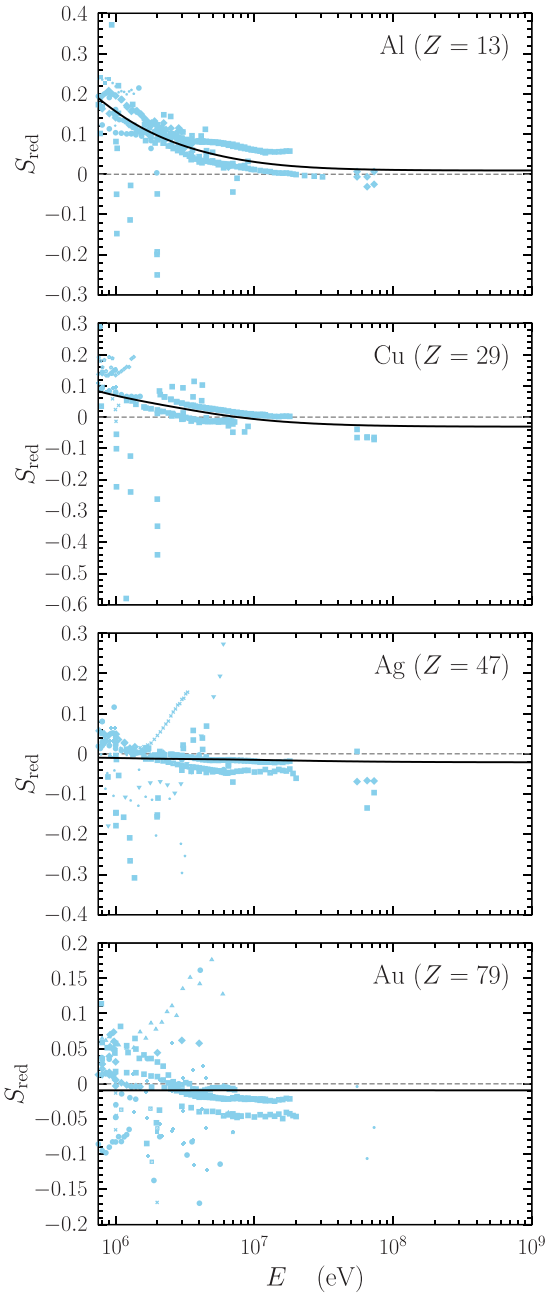

FIG. 8. Reduced stopping powers of solid aluminium, copper, silver, and gold for protons. Special symbols are values derived from the stopping powers in the IAEA database, with data from each source designated by the same symbol. The solid curves represent the function $\mathcal{G}(E)$ obtained with the fitted values of I'_0 and $C_{\rm B}$.

The fitting procedure consisted in minimizing the function

$$\chi_1^2(I'_0, C_{\rm B}) \equiv \sum_k [\mathcal{G}(E_k) - S_{\rm red}(E_k)]^2, \tag{132}$$

where E_k denote the energies of data available for each element and projectile kind, by means of the simplex method of Nelder and Mead [66], which was modified to restrict the variable domains. The calculation yielded the values of I'_0 and $C_{\rm B}$ at a relative minimum, with I'_0 in the restricted interval $(I_{\rm ICRU} - \Delta I_{\rm ICRU}, I_{\rm ICRU} + \Delta I_{\rm ICRU})$, where $\Delta I_{\rm ICRU}$ is the estimated uncertainty of the $I_{\rm ICRU}$ value taken from the ICRU Report 37 [20], and with $C_{\rm B} \in (0.5, 10)$.

With the parameters resulting from the fit, the corrected Bethe formula was found to approximate the measured stopping powers satisfactorily for projectiles with energies higher than $E_{\rm cut}$. Although the fit was judged to be uncertain due to experimental uncertainties, it revealed that the $C_{\rm B}$ parameter should increase with the atomic number of the medium, i.e., that the effect of the Barkas correction decreases when Z increases, becoming imperceptible for large Z (see Fig. 8). It was estimated that the value

$$C_{\rm B} = \max\{1, Z/10\} \tag{133}$$

is appropriate for practical calculations. In the comparisons of calculated and measured stopping powers reported below, we use this $C_{\rm B}$ value and we set $I'_0 = I_{\rm ICRU}$, which is considered to be the most realistic value available.

In order to delineate the tendency of the measured stopping powers at low energies, and also to validate the corrected Bethe formula at intermediate energies, we parametrize the stopping power for low-energy projectiles by using the empirical formula adopted in the ICRU Report 49 [39], and attributed there to Andersen and Ziegler:

$$S_{\rm low}(E) = \frac{s_{\rm l}(T)\, s_{\rm h}(T)}{s_{\rm l}(T) + s_{\rm h}(T)} \tag{134}$$

with

$$s_{\rm l}(T) = a_1 T^{a_2} \tag{135a}$$

and

$$s_{\rm h}(T) = \frac{a_3}{T} \ln\left(1 + \frac{a_4}{T} + a_5 T\right) \tag{135b}$$

where a_1, ..., a_5 are adjustable parameters. The variable T is the kinetic energy E of the projectile in units of keV for protons and in units of MeV for alphas. The parameters a_i were determined from a least-squares fit of the function (134) to the stopping powers $S_{\rm exp}(E_k)$ given in the IAEA database with $E_k \in (10\ {\rm keV}, 2E_{\rm cut})$. They were obtained, for each material and projectile kind, by minimizing the function

$$\chi_2^2(a_1, \ldots, a_5) = \sum_k [S_{\rm low}(E_k) - S_{\rm exp}(E_k)]^2 \tag{136}$$

where the summation is over the data with energies E_k in the considered interval. The minimization was performed by using the simplex method of Nelder and Mead [66]. As the parametrization (134) is used here merely as a visual device, we have not attempted to set a table of the fitted parameters and to devise suitable interpolations or extrapolations to other elements.

Generally, the fitted formula (134) and the corrected Bethe formula (with $I'_0 = I_{\rm ICRU}$ and $C_{\rm B} = \max\{1, Z/10\}$) do not yield the same values at $E_{\rm cut}$. To obtain a continuous function of the projectile's kinetic energy E, with a gradual transition from the low-E fit to the high-energy Bethe formula (128), we set

$$S(E) = \begin{cases} S_{\rm low}(E) & \text{if } E \leqslant E_{\rm cut}, \\ S_{\rm mix}(E) & \text{if } E_{\rm cut} < E \leqslant 2E_{\rm cut}, \\ S_{\rm cB}(E) & \text{if } E > 2E_{\rm cut}, \end{cases} \tag{137}$$

with

$$S_{\rm mix}(E)=\left[1-\left(\frac{E}{E_{\rm cut}}-1\right)\left(1-\frac{S_{\rm cB}(2E_{\rm cut})}{S_{\rm low}(2E_{\rm cut})}\right)\right]S_{\rm low}(E) \quad (138)$$

where $S_{\rm cB}(E)$ is the value obtained from the corrected Bethe formula (128).

Figure 9 shows a comparison of stopping powers calculated from the composite function (137) and measured values in the IAEA database for protons and alphas, limited to those elemental materials for which there were enough data with kinetic energies above $E_{\rm cut}$ to make the comparison meaningful for both protons and alphas. The IAEA data are displayed as special sky-blue symbols, different for each separate source, and the result from expression (137) is represented as a solid curve. The dashed red vertical line at the energy $E_{\rm cut}/2$ indicates the start of the plot of the corrected Bethe formula (shown as a dashed red curve), which is seen to be effectively valid for energies larger than $E_{\rm cut}$. The low-energy formula (134) is displayed as a blue dashed curve up to the energy $2E_{\rm cut}$ (indicated by the blue dashed vertical line), the double of the upper limit of the interval considered in the fit, to reveal either the consistency or the difference between its extrapolation and the corrected Bethe formula. It is seen that the low-energy and the Bethe formulas generally differ little in the interval $(E_{\rm cut}, 2E_{\rm cut})$ affected by their joining, Eq. (137).

The results displayed in Fig. 9 show that there is close agreement between the predictions of the corrected Bethe formula (with $I_0'=I_{\rm ICRU}$ and $C_{\rm B}=\max\{1,Z/10\}$) and the measurements for $E>E_{\rm cut}$. Further comparisons shown in the documentation of the Supplemental Material [21] reveal similar agreement for the other elemental materials in the IAEA database, for which the variety of available experimental data is more limited. This general agreement gives support to our calculation scheme of the Barkas correction (and the density-effect correction) from the semiempirical DHFS-model OOS, and justifies the consistency of the theory. The fact that the corrected Bethe formula is effectively determined by a single parameter, the mean excitation energy I_0', which can be identified with the I values recommended in the ICRU Report 37 [20], makes the present approach particularly amenable for practical uses.

Although the previous analysis has been limited to elemental materials, it can readily be generalized to compounds (and mixtures) by using the additivity approximation, i.e., by assuming that the molecular cross section can be approximated as the sum of atomic cross sections of the atoms in a molecule. Let us consider a compound the molecules of which consist of n_j atoms of the element of atomic number Z_j. According to the additivity approximation, the OOS of a molecule is the sum of the OOSs of its atoms and, consequently, the I value of the compound is given by

$$Z\ln I=\sum_j n_j Z_j \ln(I_j) \quad \text{with} \quad Z=\sum_j n_j Z_j, \qquad (139)$$

where I_j denotes the mean excitation energy of the element with atomic number Z_j. Since the additivity approximation neglects the effect of aggregation on the atomic OOSs, the I value resulting from Eq. (139) may differ appreciably from the "true" mean excitation energy of the material. A better estimate of the I value can only be obtained either from stopping measurements or from knowledge of the optical dielectric function of the material. The DHFS-model OOS of the compound material can be built as described in Sec. VIII, with the OOS of inner subshells (with $U_i>W_{\rm th}$) obtained by adding the contributions of the various elements present weighted by their corresponding stoichiometric indices, n_i, plus the outer-electron contribution described by the oscillator OOS, Eq. (124). The shell correction of the compound is obtained as the weighted sum of the DHFS atomic shell corrections. Naturally, the Lindhard-Sørensen correction is independent of the material composition. The density-effect and the Barkas corrections are calculated from the DHFS-model OOS of the compound. The cutoff impact parameter a, which determines the Barkas correction, may be estimated from Eq. (100) with

$$C_{\rm B}=\max\{1,\overline{Z}/10\} \quad \text{with} \quad \overline{Z}=Z\left(\sum_j n_j\right)^{-1}. \qquad (140)$$

To test the reliability of the corrected Bethe formula for compounds, with its corrections evaluated by following the proposed scheme, we consider the case of water, a compound of basic interest in dosimetry studies. In the calculation we use the empirical value of the mean excitation energy recommended in the ICRU Report 90 [67], $I_0'=78$ eV. Figure 10 compares experimental stopping cross sections (per molecule) of ice and liquid water given in the IAEA database for protons and alpha particles with the predictions of the corrected Bethe formula (128) and with the low-energy fits (134). This comparison indicates that the corrected Bethe formula, as implemented in the present calculations, provides reliable results also for compounds.

X. SUMMARY AND CONCLUDING COMMENTS

We have presented the theory of electronic stopping of materials for fast charged particles, which leads to the Bethe formula and its corrections. We have set an accurate parametrization of the Lindhard-Sørensen correction for point projectiles, as an extension of the familiar Bloch correction, and we have computed accurately and parametrized the functions $I_1(\xi)$ and $I_2(\xi)$ that enter into the calculation of the Barkas correction. On the basis of a complete database of atomic GOSs, calculated from an independent-electron model with the DHFS self-consistent potential, modifications of the Bethe formula were introduced to account for relativistic departures from the Bethe sum rule, and atomic shell corrections were calculated for all the elements with $Z=1$–99 [8]. Since the largest contribution to the shell correction comes from the innermost electron subshells, these DHFS shell corrections are assumed to be applicable also to molecules and dense materials.

A simple empirical method has been devised to build the OOSs of arbitrary materials from the subshell OOSs obtained from DHFS calculations for free atoms [8]. The resulting OOS model is determined by a single parameter, the mean excitation energy. After verifying that the details of the adopted OOS model have a minor impact on the Barkas and density-effect corrections, we have analyzed the possibility of obtaining the basic parameters of the theory, I_0' and $C_{\rm B}$, by

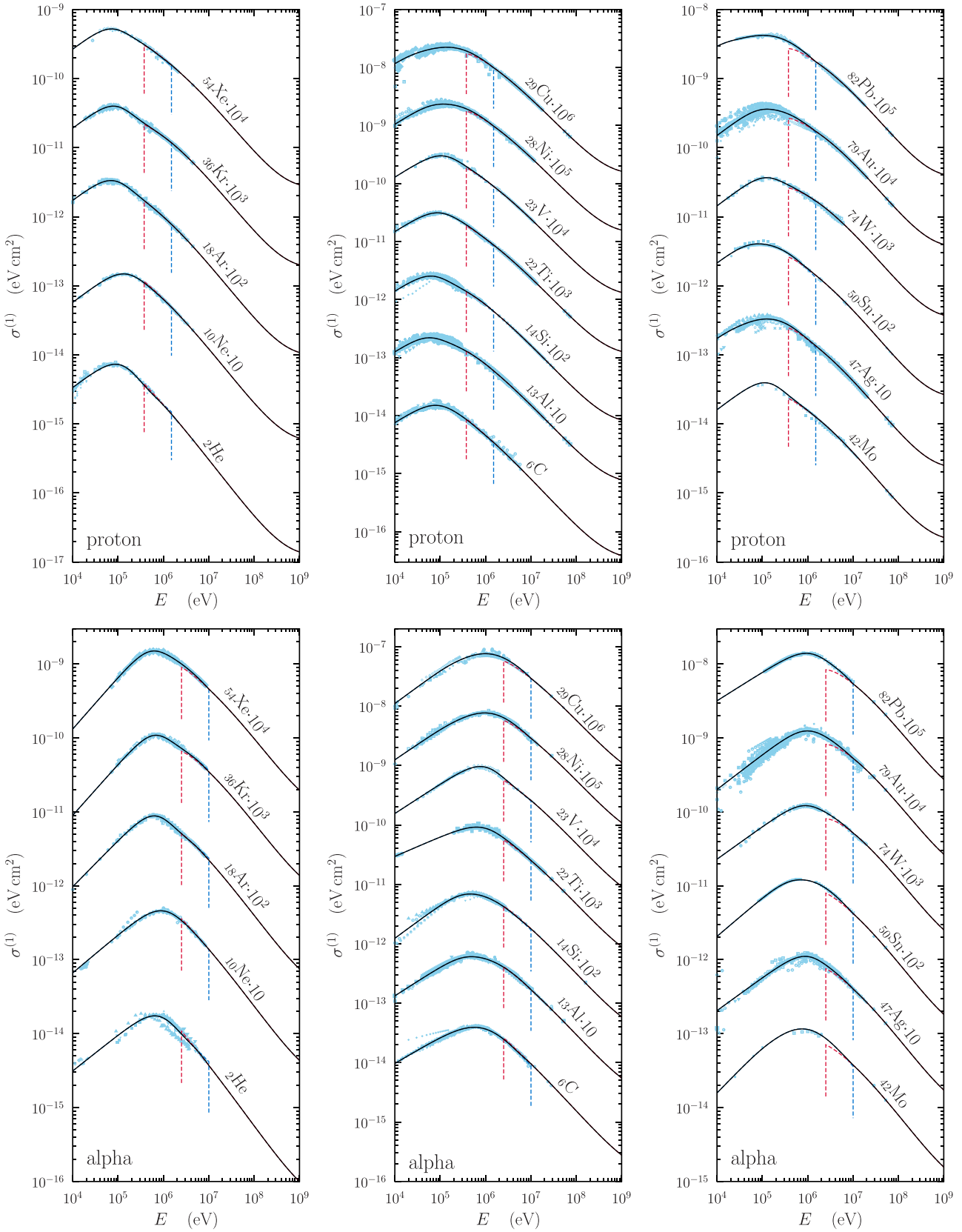

FIG. 9. Comparison of experimental stopping cross sections (per atom) from the IAEA database (symbols) with results from the composite formula (137) for protons (top) and alphas (bottom) in noble gases (left) and in elemental solids (center and right). For the sake of clarity, the displayed stopping cross sections are multiplied by the indicated powers of 10. Other details are described in the text.

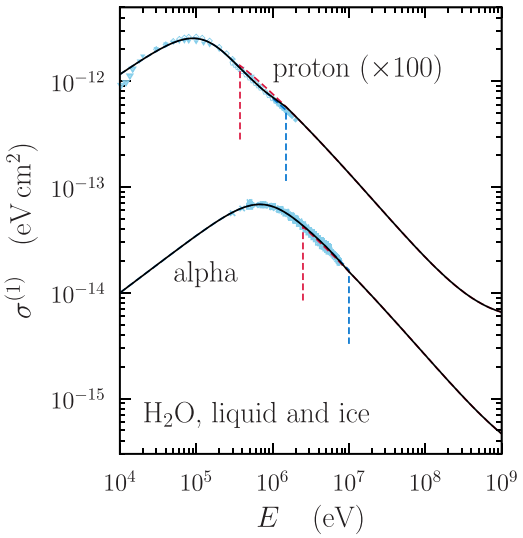

FIG. 10. Comparison of stopping cross sections (per molecule) calculated from the corrected Bethe formula for protons and alpha particles in liquid water with experimental data from the IAEA database, for both ice and liquid water. Details are the same as in Fig. 9.

fitting to experimental data, and concluded that such a process is unreliable because of experimental uncertainties.

We have verified that the corrected Bethe formula is valid for protons and alpha particles with kinetic energies higher than $E_{\rm cut} = 0.75$ MeV for protons and $= 5$ MeV for alphas. An unexpected result from the present paper is the finding that the Bethe formula, with the DHFS shell correction, the Lindhard-Sørensen correction, and the Barkas and the density-effect corrections calculated from the semiempirical DHFS-model OOS, provides results in close agreement with measured stopping powers of elemental materials from the IAEA database when I_0' is set equal to the empirical I values recommended in the ICRU Report 37 [20] and $C_{\rm B} = \max\{1, Z/10\}$. The natural extension of this prescription to compounds, based on the additivity approximation, is expected to be equally reliable, provided a realistic I value is known for the material. In the important case of water, the corrected Bethe formula, with the value $I_0' = 78$ eV recommended in the ICRU Report 90 [67], has been shown to yield results in acceptable agreement with the measurements included in the IAEA database.

The dependence of the corrected Bethe formula on a single parameter is an attractive characteristic of the proposed approach. However, the usefulness of the formula rests on the availability of a realistic I value for the considered material. Although the I values recommended in the ICRU Report 37 [20] for the elements seem to be reliable enough, this parameter may not be available for other materials. It is worth keeping in mind that the I value is strongly dependent on the OOS for low-W excitations, which is determined not only by the composition but also by the structure (aggregation state) of the material. For this reason, in the case of compounds, the additivity approximation, Eq. (139), is not expected to give reliable I values. Although empirical considerations may be helpful for estimating the I values of certain compounds (see, e.g., Ref. [20]), this fundamental parameter can only be determined unambiguously from measurements of the stopping power, which are scarce and generally affected by considerable uncertainties. The accuracy of practical dosimetry calculations still depends heavily on the reliability of available experimental stopping-power data.

A computer program implementing the present calculation scheme is made available as part of the Supplemental Material [21]. The program utilizes physical data and I values for the elements $Z = 1$–99 and for 181 compounds and mixtures taken from the database of the ESTAR program of Berger [68]. Although the I value assigned by the program is consistent with the recommendations in the ICRU Report 37 [20], the user has the option of changing it. The program also uses atomic shell corrections and subshell OOSs calculated with the DHFS potential, which are read from a numerical database included in the distribution package.

ACKNOWLEDGMENTS

I am indebted to Pedro Andreo for many enlightening discussions and for critically reading the paper. In the early development of this work I received valuable information and much advice from Hans Bichsel and Mitio Inokuti. Financial support from the Spanish Ministerio de Ciencia, Innovación y Universidades/Agencia Estatal de Investigación/European Regional Development Fund, European Union (Project No. RTI2018-098117-B-C22), is gratefully acknowledged.

[1] N. Bohr, On the theory of the decrease of velocity of moving electrified particles on passing through matter, Philos. Mag. **25**, 10 (1913).

[2] N. Bohr, On the decrease of velocity of swiftly moving electrified particles in passing through matter, London, Edinburgh, Dublin Philos. Mag. J. Sci. **30**, 581 (1915).

[3] H. A. Bethe, Zur Theorie des Durchgangs schneller Korpuskularstrahlen durch Materie, Ann. Phys. (Leipzig) **397**, 325 (1930).

[4] H. A. Bethe, Bremsformel für Elektronen relativistischer Geschwindigkeit, Z. Phys. **76**, 293 (1932).

[5] U. Fano, Penetration of protons, alpha particles and mesons, Annu. Rev. Nucl. Sci. **13**, 1 (1963).

[6] M. Inokuti, Inelastic collisions of fast charged particles with atoms and molecules: The Bethe theory revisited, Rev. Mod. Phys. **43**, 297 (1971).

[7] D. Bote and F. Salvat, Calculations of inner-shell ionization by electron impact with the distorted-wave and plane-wave Born approximations, Phys. Rev. A **77**, 042701 (2008).

[8] F. Salvat, L. Barjuan, and P. Andreo, Inelastic collisions of fast charged particles with atoms. Bethe asymptotic formulas and shell corrections, Phys. Rev. A **105**, 042813 (2022).

[9] E. Fermi, The ionization loss of energy in gases and in condensed materials, Phys. Rev. **57**, 485 (1940).

[10] J. Lindhard, On the properties of a gas of charged particles, Dan. Mat. Fys. Medd. **28**, 1 (1954).

[11] J. D. Jackson, *Classical Electrodynamics*, 2nd ed. (Wiley, New York, 1975)

[12] U. Fano, Atomic theory of electromagnetic interactions in dense materials, Phys. Rev. **103**, 1202 (1956).

[13] M. Inokuti and D. Y. Smith, Fermi density effect on the stopping power of metallic aluminum, Phys. Rev. B **25**, 61 (1982).

[14] F. Bloch, Zur Bremsung rasch bewegter Teilchen beim Durchgang durch Materie, Ann. Phys. (Leipzig) **408**, 285 (1933).

[15] J. Lindhard and A. H. Sørensen, Relativistic theory of stopping for heavy ions, Phys. Rev. A **53**, 2443 (1996).

[16] J. Ashley, R. H. Ritchie, and W. Brandt, Z_1^3 effect in the stopping power of matter for charged particles, Phys. Rev. B **5**, 2393 (1972).

[17] J. D. Jackson and R. L. McCarthy, Z_1^3 corrections to energy loss and range, Phys. Rev. B **6**, 4131 (1972).

[18] This database is available from the IAEA web site, https://www-nds.iaea.org/stopping/index.html. The data used in the present paper were downloaded in March 2022.

[19] C. C. Montanari and P. Dimitriou, The IAEA stopping power database, following the trends in stopping power of ions in matter, Nucl. Instrum. Methods Phys. Res., Sect. B **408**, 50 (2017).

[20] ICRU Report 37, *Stopping Powers for Electrons and Positrons* (ICRU, Bethesda, 1984).

[21] See Supplemental Material at http://link.aps.org/supplemental/10.1103/PhysRevA.106.032809 for additional comparisons of stopping powers predicted by the corrected Bethe formula and experimental data for other elements in the IAEA database. Also included are the Fortran program CBETHE, which implements the formula and corrections described in the text, and its associated databases.

[22] N. Bohr, The penetration of atomic particles through matter, K. Dan. Vidensk. Selsk. Mat. Fys. Medd. **18**, 1 (1948).

[23] S. P. Ahlen, Theoretical and experimental aspects of the energy loss of relativistic heavily ionizing particles, Rev. Mod. Phys. **52**, 121 (1980).

[24] N. F. Mott, The scattering of fast electrons by atomic nuclei, Proc. R. Soc. A **124**, 425 (1929).

[25] N. F. Mott and H. S. W. Massey, *The Theory of Atomic Collisions* (Oxford University, London, 1965).

[26] W. A. McKinley and H. Feshbach, The Coulomb scattering of relativistic electrons by nuclei, Phys. Rev. **74**, 1759 (1948).

[27] D. Griffiths, *Introduction to Quantum Mechanics* (Prentice-Hall, Upper Saddle River, NJ, 1995).

[28] F. Olver, D. Lozier, R. Boisvert, and C. Clark, *NIST Handbook of Mathematical Functions* (Cambridge University, New York, 2010), print companion to the NIST Digital Library of Mathematical Functions, http://dlmf.nist.gov/.

[29] B. H. Bransden and C. J. Joachain, *Physics of Atoms and Molecules* (Longman Scientific&Technical, Harlow UK, 1983).

[30] C. Møller, Zur theorie des durchgangs schneller elektronen durch materie, Ann. Phys. (Leipzig) **406**, 531 (1932).

[31] F. Salvat and J. M. Fernández-Varea, RADIAL: A Fortran subroutine package for the solution of the radial Schrödinger and Dirac wave equations, Comput. Phys. Commun. **240**, 165 (2019); see also the manual of the computer code.

[32] P. Sigmund, *Particle Penetration and Radiation Effects* (Springer-Verlag, Berlin, 2006).

[33] R. M. Sternheimer, The density effect for the ionization loss in various materials, Phys. Rev. **88**, 851 (1952).

[34] R. M. Sternheimer, S. M. Seltzer, and M. J. Berger, Density effect for the ionization loss of charged particles in various substances, Phys. Rev. B **26**, 6067 (1982).

[35] C. J. Joachain, *Quantum Collision Theory* (North-Holland, Amsterdam, 1975).

[36] J. Lindhard, The Barkas effect—or Z_1^3, Z_1^4—corrections to stopping of swift charged particles, Nucl. Instrum. Methods **132**, 1 (1976).

[37] J. C. Ashley, Optical-data model for the stopping power of condensed matter for protons and antiprotons, J. Phys.: Condens. Matter **3**, 2741 (1991).

[38] J. F. Ziegler, The stopping of energetic light ions in elemental matter, J. Appl. Phys. **85**, 1249 (1999).

[39] ICRU Report 49, *Stopping Powers and Ranges for Protons and Alpha Particles* (ICRU, Bethesda, 1993).

[40] J. S. Levinger, M. L. Rustgi, and K. Okamoto, Relativistic corrections to the dipole sum rule, Phys. Rev. **106**, 1191 (1957).

[41] S. M. Cohen and P. T. Leung, General formulation of the semirelativistic approach to atomic sum rules, Phys. Rev. A **57**, 4994 (1998).

[42] S. M. Cohen, Bethe stopping power theory for heavy-element targets and relativistic projectiles, Phys. Rev. A **68**, 012720 (2003).

[43] S. M. Cohen, Range of validity for perturbative treatments of relativistic sum rules, Phys. Rev. A **68**, 042704 (2003).

[44] S. Tanuma, C. J. Powell, and D. R. Penn, Calculations of electron inelastic mean free paths. VIII. Data for 15 elemental solids over the 50–2000 eV range, Surf. Interface Anal. **36**, 1 (2004).

[45] J. M. Fernández-Varea, F. Salvat, M. Dingfelder, and D. Liljequist, A relativistic optical-data model for inelastic scattering of electrons and positrons in condensed matter, Nucl. Instrum. Methods Phys. Res., Sect. B **229**, 187 (2005).

[46] J. M. Fernández-Varea, D. Liljequist, S. Csillag, R. Räty, and F. Salvat, Monte Carlo simulation of 0.1–100 keV electron and positron transport in solids using optical data and partial wave methods, Nucl. Instrum. Methods Phys. Res., Sect. B **108**, 35 (1996).

[47] D. R. Penn, Electron mean-free-path calculations using a model dielectric function, Phys. Rev. B **35**, 482 (1987).

[48] I. Abril, R. García-Molina, C. D. Denton, F. J. Pérez-Pérez, and N. R. Arista, Dielectric description of wakes and stopping powers in solids, Phys. Rev. A **58**, 357 (1998).

[49] B. Da, H. Shinotsuka, H. Yoshikawa, Z. J. Ding, and S. Tanuma, Extended Mermin Method for Calculating the Electron Inelastic Mean Free Path, Phys. Rev. Lett. **113**, 063201 (2014).

[50] E. Shiles, T. Sasaki, M. Inokuti, and D. Y. Smith, Self-consistency and sum-rule tests in the Kramers-Kronig analysis of optical data: Applications to aluminum, Phys. Rev. B **22**, 1612 (1980).

[51] *Handbook of Optical Constants of Solids*, edited by E. D. Palik (Academic, New York, 1985), Vol. 1.

[52] *Handbook of Optical Constants of Solids*, edited by E. D. Palik (Academic, New York, 1991), Vol. 2.

[53] *Handbook of Optical Constants of Solids*, edited by E. D. Palik (Academic, New York, 1998), Vol. 3.

[54] R. F. Egerton, *Electron Energy-Loss Spectroscopy in the Electron Microscope*, 3rd ed. (Springer, New York, 2011).

[55] W. S. M. Werner, K. Glantschnig, and C. Ambrosch-Draxl, Optical constants and inelastic electron-scattering data for 17 elemental metals, J. Phys. Chem. Ref. Data **38**, 1013 (2009).

[56] B. L. Henke, E. M. Gullikson, and J. C. Davis, X-ray interactions: Photoabsorption, scattering, transmission, and reflection at $E = 50$–$30{,}000$ eV, $Z = 1$–92, At. Data Nucl. Data Tables **54**, 181 (1993).

[57] B. L. Henke, E. M. Gullikson, and J. C. Davis, Low-energy X-ray Interaction Coefficients: Photoabsorption, Scattering, and Reflection, $E = 30$–$30{,}000$ eV, $Z = 1$–92, Lawrence Berkeley Laboratory, Berkeley, CA (2010), available from https://github.com/praxes/henke_physical_reference.

[58] L. D. Landau and E. M. Lifshitz, *The Classical Theory of Fields*, 3rd revised English ed. (Pergamon, London, 1971).

[59] J. Lindhard and M. Scharff, Energy loss in matter by charged particles of low charge, Dan. Mat. Fys. Medd. **27**, 1 (1953).

[60] R. E. Johnson and M. Inokuti, The local-plasma approximation to the oscillator-strength spectrum: How good is it and why? Comments At. Mol. Phys. **14**, 19 (1983).

[61] C. J. Tung, R. L. Shyu, and C. M. Kwei, Mean excitation energies of atoms using the local plasma approximation, J. Phys. D **21**, 1125 (1988).

[62] G. Molière, Theorie der Streuung schneller geladener Teilchen I: Einzelstreuung am abgeschirmten Coulomb-Feld, Z. Naturforsch. **2**, 133 (1947).

[63] C. C. Montanari and J. E. Miraglia, The dielectric formalism for inelastic processes in high-energy ion-matter collisions, Adv. Quantum Chem. **65**, 165 (2013).

[64] T. A. Carlson, *Photoelectron and Auger Spectroscopy* (Plenum, New York, 1975).

[65] J. J. Rehr and R. C. Albers, Theoretical approaches to x-ray absorption fine structure, Rev. Mod. Phys. **72**, 621 (2000).

[66] J. Nelder and R. Mead, A simplex method for function minimization, Comput. J. **7**, 308 (1965).

[67] ICRU Report 90, *Key Data for Ionizing-Radiation Dosimetry: Measurement Standards and Applications* (ICRU, Bethesda, 2016).

[68] M. J. Berger, ESTAR, PSTAR and ASTAR: Computer programs for calculating stopping-power and range tables for electrons, protons and helium ions, NIST Technical Report No. 4999, 1992.